




2018

STABILITY IMPROVEMENTS FOR GENERALIZED AVERAGE-VALUE MODEL OF DC-DC CONVERTERS

Mahsen Salah Al-Ani

University of Kentucky, mahsen.al-ani@uky.edu

Author ORCID Identifier:

 <https://orcid.org/0000-0002-7171-4647>

Digital Object Identifier: <https://doi.org/10.13023/etd.2018.296>

[Right click to open a feedback form in a new tab to let us know how this document benefits you.](#)

Recommended Citation

Al-Ani, Mahsen Salah, "STABILITY IMPROVEMENTS FOR GENERALIZED AVERAGE-VALUE MODEL OF DC-DC CONVERTERS" (2018). *Theses and Dissertations--Electrical and Computer Engineering*. 121.
https://uknowledge.uky.edu/ece_etds/121

This Master's Thesis is brought to you for free and open access by the Electrical and Computer Engineering at UKnowledge. It has been accepted for inclusion in Theses and Dissertations--Electrical and Computer Engineering by an authorized administrator of UKnowledge. For more information, please contact UKnowledge@lsv.uky.edu.

STUDENT AGREEMENT:

I represent that my thesis or dissertation and abstract are my original work. Proper attribution has been given to all outside sources. I understand that I am solely responsible for obtaining any needed copyright permissions. I have obtained needed written permission statement(s) from the owner(s) of each third-party copyrighted matter to be included in my work, allowing electronic distribution (if such use is not permitted by the fair use doctrine) which will be submitted to UKnowledge as Additional File.

I hereby grant to The University of Kentucky and its agents the irrevocable, non-exclusive, and royalty-free license to archive and make accessible my work in whole or in part in all forms of media, now or hereafter known. I agree that the document mentioned above may be made available immediately for worldwide access unless an embargo applies.

I retain all other ownership rights to the copyright of my work. I also retain the right to use in future works (such as articles or books) all or part of my work. I understand that I am free to register the copyright to my work.

REVIEW, APPROVAL AND ACCEPTANCE

The document mentioned above has been reviewed and accepted by the student's advisor, on behalf of the advisory committee, and by the Director of Graduate Studies (DGS), on behalf of the program; we verify that this is the final, approved version of the student's thesis including all changes required by the advisory committee. The undersigned agree to abide by the statements above.

Mahsen Salah Al-Ani, Student

Dr. Aaron Cramer, Major Professor

Dr. Aaron Cramer, Director of Graduate Studies

STABILITY IMPROVEMENTS FOR GENERALIZED AVERAGE-VALUE
MODEL OF DC-DC CONVERTERS

THESIS

A thesis submitted in partial fulfillment
of the requirements for the degree of
Master of Science in Electrical
Engineering in the College of Engineering
at the University of Kentucky

By

Mahsen Salah Al-Ani

Lexington, Kentucky

Director: Dr. Aaron Cramer, Associate Professor and Director of Graduate
Studies, Department of Electrical and Computer Engineering, Lexington,
Kentucky 2018

Copyright©2018 Mahsen S. Al-Ani

ABSTRACT OF THESIS

STABILITY IMPROVEMENTS FOR GENERALIZED AVERAGE-VALUE MODEL OF DC-DC CONVERTERS

Power electronics have a significant role in modern electrical devices, for instance, hybrid electric vehicles. Power electronics are the technology in between the source and the load circuits and can convert the power from dc to ac or from dc to ac. There are also many types of dc-dc converters, like such as boost and buck converters, which exhibit switching ripple behavior. A boost converter increases the output voltage (with respect to the input voltage) and reduces the output current. A buck converter decreases the output voltage and increases the output current. Many models are used to predict the behavior of the boost and buck converters. The detailed (DET), state-space averaged (SSA), and generalized averaging method (GAM) models are capable of predicting the average behavior of dc-dc converters. For DET and GAM models, the rippling behavior can also be predicted. These models differ in terms of required run time, existence of constant equilibrium points, and accuracy. The DET model has a long run time and does not have constant equilibrium, but it is very accurate. The SSA technique is a mathematical and time-invariant model that capable of describing the behavior of a dc-dc boost converters. It can derive the small signal ac equations of a switching converter and is used to illustrate the average behavior of any linear or nonlinear system in converters. The SSA does not take extensive runtime simulation and has constant equilibrium points, and can be applied to continuous, discrete and sample data systems. The GAM model can predict the average and ripple behavior in power electronic systems and has constant equilibrium and fast run time. However, it has a numerical stability issue. The integrator stabilized multifrequency averaging (ISMFA) model is employed to solve the stability issue in the GAM model, but it is a complicated dynamic method and has restrictions in its process. In the present study, a simplified but stable GAM model is introduced to predict the average and ripple behavior of boost dc-dc converters and to overcome the limitations of other methods. In this work, the stabilized GAM model has been used for a dc-dc boost converters. The stability of the proposed model is analyzed. The performance of the improved GAM model is compared with the DET, SSA, and GAM models. The results show that the stabilized GAM model is stable with the additional poles created by the GAM assignable by parameter choice. The new GAM model predicts the same results as the existing GAM method without the underlying stability concerns. The stabilized GAM model exhibits constant

equilibrium point and requires significantly lower run times than the DET model, but it is also able to predict the ripple performance of the converter. The stabilized GAM model does not take a long run time, is less complicated, has fewer restrictions, has constant equilibrium and internal stability, and has more straightforward implementation than other models, like the ISMFA model. It represents a suitable alternative to DET models when high accuracy simulations are desired without long simulation run times.

KEYWORDS: DC-DC Converter, Modelling, Power Electronic Systems, Pulse Width Modulation, Stability.

Author's signature: Mahsen S. Al-Ani

Date: July 25, 2018

STABILITY IMPROVEMENTS FOR GENERALIZED AVERAGE-VALUE
MODEL OF DC-DC CONVERTERS

By
Mahsen S. Al-Ani

Director of Thesis: Dr. Aaron Cramer

Director of Graduate Studies: Dr. Aaron Cramer

Date: July 25, 2018

DEDICATION

To my dad—the light of my eyes; the person who gives me confidence, support, safety; and encourages me to continue my educational journey. You have offered me your unwavering mental and emotional support, loved me, and made the difficult easy, sacrificed and worked late into the night to support my dream of obtaining a higher degree.

To my mum—the one who showers me with affection, kindness and love, stays up late praying for my success and happiness in life, knows my feelings without me telling her, and calls to cheer me up during difficult times. You are there for me to talk to anytime, and you give me hope in life; you bears hardships in life for my comfort, and taught me how to be patient.

To my husband—the man who gives me love, stands by me through the life's difficulties, encourages me to be successful and happy, and has spent countless hours making my life easier. To the person whose care for me never ceases.

To my brothers—my second set of eyes and support in life, to the people who remind me to trust in Allah, and for being so worthy of the pride I have in them.

To my sisters—the ones I cannot live without. You are my life role models who are pure in heart. You have taught me to overlook my hardships and focus on the blessings.

To my sons—my heart and my soul. You were so patient with me as I worked to complete my degree, and I will never stop loving you.

To my relatives and friends—for being there for me. you helped me forget my struggles, prayed for me, and always let me know you cared.

To all the people in my life who have touched my heart,
this thesis is dedicated to you
Thank you.

ACKNOWLEDGEMENTS

First, praises and thanks to Allah, the Almighty, for His showers of blessings throughout my research work to complete the research successfully. I owe it all to Almighty God for granting me the wisdom, health and strength to undertake this research task and enabling me to its completion.

I would like to thank my advisor, Dr. Aaron Cramer, whose guidance made the completion of this study possible. Thank you for providing invaluable mentorship, and direction throughout this thesis project. My deepest gratitude goes out to you.

I cannot express enough thanks to my committee for their continued support, encouragement, and many hours of their time. Many thanks to my committee: Dr. Yaun Liao, Dr. Dan Ionel, and my committee chair, Dr. Aaron Cramer. I offer my sincere appreciation for the incredible learning opportunities you have provided.

My deepest gratitude also goes to my caring, loving, and supportive husband, Ahmed. You offered encouragement when the times got rough, took over household responsibilities, and offered advice all while having a busy schedule of your own. You led me through the valley of darkness with the light of hope and support.

I would also like to thank all students and faculty members of the Department of Electrical Engineering for their generous help in various ways. I would especially like to take this opportunity to say warm thanks to Dr. Janet Lumpf for support and help, and my colleague, Akeyo Oluwaseun, for all of the helpful meetings and discussions.

I owe a deep debt of gratitude to the Higher Committee for Education Development in Iraq (HCED) for their support and scholarship that have given me the opportunity to complete this work. The support and scholarship provided by HCED has been instrumental in my ability to learn and create this work, and without their help, this study would not have been possible.

Last but not least, I would also like to express my wholehearted thanks to my beloved family, relatives, and friends for their generous support throughout my entire life, and particularly through the process of pursuing this master's degree. Because of their unconditional love and prayers, I have the chance to complete this thesis.

Contents

Acknowledgements	iii
List of Figures	vii
List of Tables	viii
1 Introduction	1
1.1 The Types of Models in Power Electronics Converter	2
1.2 Thesis Outline	3
2 DC-DC Converter Background	4
2.1 The Fundamentals of the Boost Converter	4
2.1.1 The Fundamentals of The Buck Converter	6
2.2 Detailed Model of Switching Converter	8
2.3 State Space Average Model	10
2.4 Generalized Average Method	13
2.5 Definition of Fourier Series	13
2.6 The Time Derivative of Fourier Series Waveform	15
2.7 Product Average Signals in DC-DC Converter	16
2.8 The Switching Function of DC-DC converter	19
2.9 GAM Model of the DC-DC converters	20
2.9.1 The GAM Model of the Boost Converter	20
2.9.2 Using the GAM Model in the Buck Converter	21
2.10 Pulse Width Modulation in Power Electronics	22
2.11 Stability in Power Electronics	25
3 Stabilized Generalized Averaging Model in DC-DC Converters	26
3.1 Stabilized Generalized Averaging Model (SGAM)	26
3.2 Using Fourier Series in SGAM	27

3.3	Product Average Signals in DC-DC Converter	29
3.3.1	The Switching Function of Dc-Dc Converter	30
3.4	The Integrator of the Stabilized Generalized Averaging Model . . .	31
3.5	Using Stabilized Generalized Averaging Model in DC-DC Converter	33
3.5.1	The SGAM of Boost Converter	33
3.5.2	The SGAM of Buck Converter	34
3.6	Transformation to Constant Matrix (P)	35
3.7	The Stability in The SGAM integrator	37
3.8	Lyapunov Function	41
3.9	Stability in DC-DC Converter	43
4	Simulation Results	46
4.1	Introduction	46
4.1.1	Boost Converter Simulation Results	47
4.1.2	Buck Converter Simulation Results	54
5	Discussion and Conclusions	64
5.1	Discussion The Results for The Models	64
5.2	Conclusions and Future Work	66
A	Hardware DC-DC Converter in The Lab	68
	References	71
	Vita	80

List of Figures

2.1	Boost converter circuit	4
2.2	Illustrates the boost converter circuit during ON time	5
2.3	Illustrates the basic operation of the buck converter circuit	6
2.4	The buck converter during ON time	7
2.5	The buck converter circuit during OFF-state	8
2.6	The buck converter circuit during OFF-state	8
2.7	Pulse width modulation	24
3.1	The comparison the integrator of DET, GAM, and SGAM models of integrator	40
3.2	Shows the elements of x for SGAM model of integrator	40
3.3	Shows the elements of x for SGAM model of integrator	41
3.4	Time-domain signals of DET, GAM, and SGAM models of inte- grators	41
3.5	Shows the SGAM integrator model with various approximation orders in boost converter	44
3.6	Shows the SGAM integrator model with various approximation orders in buck converter	45
4.1	The Capacitor voltage for SGAM model in boost converter	48
4.2	The inductance current for SGAM model in boost converter	49
4.3	The capacitor voltage for detailed, SSA SGAM in boost converter	49
4.4	The inductance current for detailed, SSA SGAM in boost converter	50
4.5	The capacitor voltage for Detailed,SSA,and SGAM models in boost converter	50
4.6	The inductor current for Detailed,SSA,and SGAM models in boost converter	51
4.7	The Capacitor voltage for GAM and SGAM model in boost con- verter	51

4.8	The inductance current for GAM and SGAM models in boost converter	52
4.9	The capacitor voltage for GAM and SGAM models in boost converter	52
4.10	The inductor current for GAM and SGAM models in boost converter	53
4.11	The capacitor voltage of SGAM in buck converter	55
4.12	The inductance current of SGAM in buck converter	56
4.13	Capacitor voltage of SGAM and DET model in buck converter . .	56
4.14	Inductor current of SGAM and DET model in buck converter . . .	57
4.15	Capacitor voltage of SGAM and DET model in buck converter . .	57
4.16	Inductance current of SGAM and DET model in buck converter .	58
4.17	Capacitor voltage of SGAM and SSA models in buck converter .	58
4.18	Inductance current of SGAM, DET,and GAM models in buck converter	59
4.19	The capacitor voltage for SGAM and GAM model in buck converter	59
4.20	Inductance current for SGAM and GAM model in buck converter	60
4.21	Capacitor voltage for DET,GAM and SGAM models in buck converter	61
4.22	Inductance current for DET, GAM, and SGAM models in buck converter	61
4.23	Capcitor voltage for DET, GAM, and SGAM model in buck converter	62
4.24	Inductance current for DET, GAM, and SGAM models in buck converter	62

List of Tables

3.1	Integrator Parameter	38
4.1	The Parameters of Boost Converter	48
4.2	Run time simulation for boost converter	53
4.3	Comparison of DC value and peak-peak (P-P) value of inductor current and capacitor voltage for detailed DET, SSA, GAM, and SGAM models of boost converter	54
4.4	Buck Converter Simulation Parameters	54
4.5	Run Time Simulation of Boost Converter	62
4.6	Comparison of dc value and peak-peak (P-P) value of inductor current and capacitor voltage for detailed, SSA, GAM, and SGAM models	63

Chapter 1

Introduction

Power electronic systems have become very popular in the recent times. Power electronic are the technology in between the source and the load circuits and can convert the power from dc or ac to dc or ac in both directions. Power electronic converters consist of four kinds: it can be converted ac-to-dc converter such as rectifiers, dc to ac converter like inverter, dc to dc converter such as chopper, and ac to ac converter likes cycloconverter. In the electrical devices, power electronic converters have an essential role in increasing operational efficiency, faster dynamics, and small sizes compared to mechanical systems for similar power ratings. Power electronic applications are found in industry appliances, such as aircrafts, automobiles, machine tools, home appliances, toys and many other products. However, they have a critical disadvantage, which is the harmonics [1–3]. Since converters are located between the sources and the loads, the harmonics will be on both sides. Harmonics are produced in the output voltage and current and the input current and cause an extreme heat, power losses and noise.

There are many other dc-dc converters such as: regular linear, buck converter, boost converter, and buck/boost converter. The dc-dc converters have several advantages: uncomplicated design, low noise, fast transient response and low cost. However, these converters have low efficiency if the input and the output have substantially different values and need a sink to dissipate heat. Boost converters have a variety of uses these days: RF, radio, communication devices, medical equipment, measurement devices, etc. A boost converter, which is called a step up-converter, increases the output voltage from its source and reduces the output current. Boost converters are widely used in hybrid electrical vehicles, regulated dc supplies, regenerative braking of dc motors or switching regulators, etc. [2, 3]. As shown in Fig.1, a boost converter circuit contains passive elements such as

a resistor, inductor, and capacitor, and has active elements; such as bipolar junction transistor (IGBTs) or metal oxide semiconductor field effect transistor (MOSFETS), and a diode, both of which act as a switch. Otherwise, the buck converter decreases the output voltage and increase the output current. A buck converter circuit is consisting of a resistor, inductor, and capacitor, and has active elements; such as (IGBTs) or (MOSFETS) transistor, and a diode as shown in Fig .4. Buck converters are widely used laptops, tablets, audio amplifiers and motor control [4].

Additionally, these converters have ripples and harmonics in the output signal, which cause noise and losses in the power. To predict the ripples in the converters, there are several types of models that will clarify next section.

1.1 The Types of Models in Power Electronics Converter

In order to predict the ripple behavior, some models were discovered and simulated in software programs. The detailed (DET), state-space averaging (SSA), and multifrequency averaging (GAM) models are able to predict the average behavior as well as the ripple behavior of power electronic systems. These models were compared based on runtime simulation and constant equilibrium. For instance, the SSA model is beneficial when the ripple is small and time-invariant [5, 6]. However, the new model, which is called stabilized generalized multifrequency method (SGAM), has been used to describe the operation in power electronics, but it has a long run time simulation and does not have constant equilibrium. Finally, the MFA model used the truncated Fourier series to analyze the state variable (inductor current and capacitor voltage) of power electronic systems. This model is capable of predicting the average behavior in power electronic systems and ripple behavior. However, it has a numerical stability issue [7]. The integrator stabilized multifrequency averaging (ISMAF) model is employed to solve the stability issue in the GAM model, but it is a complicated dynamic method and has restrictions on its process. These models still have problems such as taking a long time to obtain the output, having complicated subsystems in their model, having restrictions, not having constant equilibrium, and having instability issue. However, SGAM model does not take a long time to run, has a less complicated system, fewer restrictions, and has a constant equilibrium and stability.

The SGAM model has been used in the dc-dc converters, and it is stable while other models are not like GAM model . This model does not have a long run time in Simulink and no restrictions and has a stable output signal.

This model is capable of predicting the ripple and average behavior. It is developed through Simulink MATLAB (2017a). The results from SGAM model integrator are stable depending on the assignable parameter that are in its subsystem. Lyapunov technique has been used to prove the stability of the system [8, 9]. The switch function dc-dc converters have been analyzed in Fourier-series representation. The simulation results of SGAM model with GAM model in the boost and buck converters have been compared.

1.2 Thesis Outline

The organizing of this thesis as follows. The fundamentals of differential equation model and its properties are presented in Chapter 2. In Chapter 3, SGAM model of dc-dc converters is proposed. In Chapter 4 we present the results of simulations for the SGAM models in the dc-dc converter as carried out by the researcher. In Chapter 5, the conclusions of this research project are discussed, and potential avenues for future work are presented.

Chapter 2

DC-DC Converter Background

2.1 The Fundamentals of the Boost Converter

Power electronics has several kinds of converters and the dc-dc converter is one of these converters. The dc-dc converter has become essential for electrical devices due to the flexibility of this converter to produce different dc output voltages compared to the input voltage. The boost converter is a dc-dc converter that increases the output voltage. The boost converter is widely used in LED drivers, solar power systems, and hybrid electric vehicles [10]. The boost converter circuit consists of one transistor, one diode as a switch, inductor, one capacitor, and load such as a resistor, as shown in Fig 2.1.

The topology for the basic boost converter is set forth. When the transistor (Q1) is ON, the diode is reversed bias as shown in Fig. 2.2; therefore, the output circuit is isolated, and the inductor is charged. Therefore, the inductor stores the

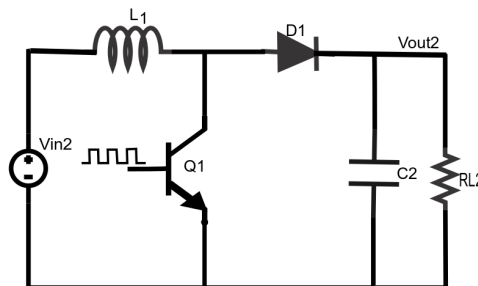


Figure 2.1: Boost converter circuit

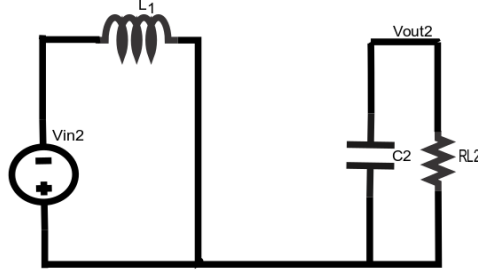


Figure 2.2: Illustrates the boost converter circuit during ON time

energy and there is no current flowing to the rest of the circuit (diode, capacitor, and load resistor). According to KVL, the inductor voltage is described as

$$L \frac{di_{L2}}{dt} = V_{in2}, \quad (2.1)$$

where L is the inductance, i_{L2} is the inductance current, and V_{in2} is the input voltage. Likewise, using KCL during the ON period of the boost converter, the capacitor current is described as

$$C_2 \frac{dv_{out2}}{dt} = -\frac{V_{out2}}{R_{L2}}, \quad (2.2)$$

where the C_2 is the capacitor, v_{out2} is the capacitor voltage, and R_{L2} is the load resistance in the boost converter. Equation 2.3 produced by combining equation 2.1 and 2.2.

$$\begin{bmatrix} \frac{di_{L2}}{dt} \\ \frac{dv_{out2}}{dt} \end{bmatrix} = \begin{bmatrix} 0 & 0 \\ 0 & -\frac{1}{R_{L2}C_2} \end{bmatrix} \begin{bmatrix} i_{L2} \\ v_{out2} \end{bmatrix} + \begin{bmatrix} \frac{1}{L} \\ 0 \end{bmatrix} V_{in2}, \quad (2.3)$$

Otherwise, when the switch (Q) is OFF and the diode is closed, the inductor current via the diode-capacitor to the load as shown in Fig. 2.6[11]. Here, the capacitor receives the energy that from the inductor and input voltage. According to KVL, the inductor voltage is described as

$$L \frac{di_{L2}}{dt} = V_{in2} - v_{out2}, \quad (2.4)$$

eq:5

where L is the inductance, V_{in2} is the input voltage, and v_{out2} is the capacitance voltage in the boost converter.

The capacitance current of boost converter by applying KCL is shown in 2.5 [4, 12]

$$C_2 \frac{dv_{out2}}{dt} = i_{L2} - \frac{V_{out2}}{R_{L2}}, \quad (2.5)$$

The general equations for boost converter can be clarified as

$$L \frac{di_{L2}}{dt} = V_{in2} - (1 - q)v_{out2}, \quad (2.6)$$

$$C_2 \frac{dv_{out2}}{dt} = (1 - q)i_{L2} - \frac{V_{out2}}{R_{L2}}, \quad (2.7)$$

The advantages of the boost converters are high efficiency, supply one polarity output voltage and easily comprehensible circuitry. However, boost converters are not often used for high power conversion.

2.1.1 The Fundamentals of The Buck Converter

The buck converter is a step-down converter and generates lower output voltage and higher current than the input. The buck converter is remarkably used in smartphones, laptops, tablets, audio amplifiers and motor control. This converter is operated in both continuous and discontinuous current mode. The buck converter circuit consists of an active switch, such as a MOSFET transistor, a passive switch, such as a diode, an inductor, a capacitor, and load, as shown in Fig. 2.3.

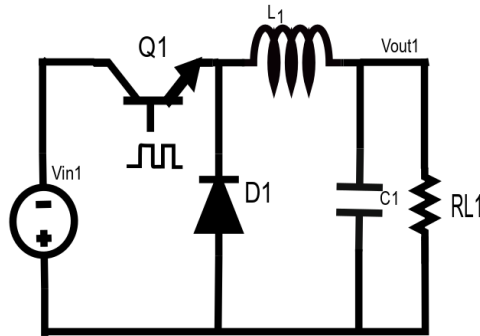


Figure 2.3: Illustrates the basic operation of the buck converter circuit

The inductor and capacitor act as a filter to reduce the ripple in the output voltage, and the MOSFET can be controlled by turning it ON or OFF. During the

ON status of the buck converter, a current loop is created as shown in Fig. 2.4. The inductor current increases linearly according to Faraday's law ($L\frac{di_L}{dt}$). Depending on KVL, the inductor voltage is obtained see equation 2.8

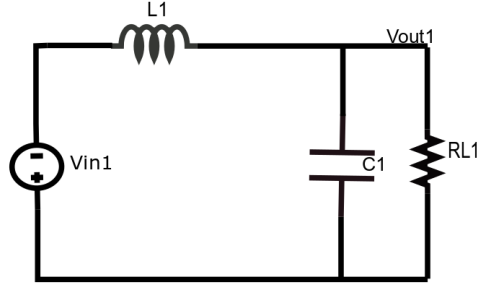


Figure 2.4: The buck converter during ON time

$$L\frac{di_{L1}}{dt} = V_{in1} - v_{out1}, \quad (2.8)$$

furthermore, by using KCL during the ON status of the buck converter; the capacitor voltage is described as

$$C_1\frac{dv_{out1}}{dt} = i_{L1} - \frac{V_{out1}}{R_{L1}}, \quad (2.9)$$

Otherwise, when the switch (Q) is OFF and the diode is closed, the inductor current flows across the diode, capacitor and load as shown in Fig. 2.5. Here, the capacitor will be charged from the energy that at the inductor, using KVL, the capacitor voltage is given in equation 2.10

$$v_L = V_D - v_{out1} \approx -v_{out1}, \quad (2.10)$$

and, the capacitance current is defined as [4]

$$C_1\frac{dv_{out1}}{dt} = i_{L1} - \frac{V_{out1}}{R_{L1}}, \quad (2.11)$$

The advantages of buck converter are high efficiency, less expensive. The general equations for buck converters can clarified as

$$C_1\frac{dv_{out1}}{dt} = i_{L1} - \frac{V_{out1}}{R_{L1}}, \quad (2.12)$$

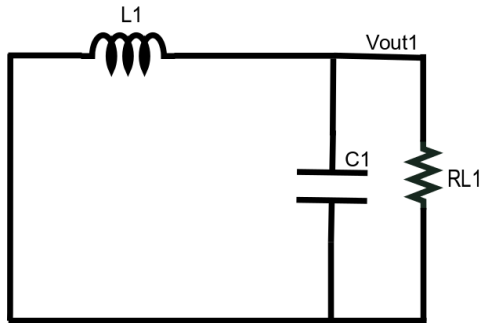


Figure 2.5: The buck converter circuit during OFF-state

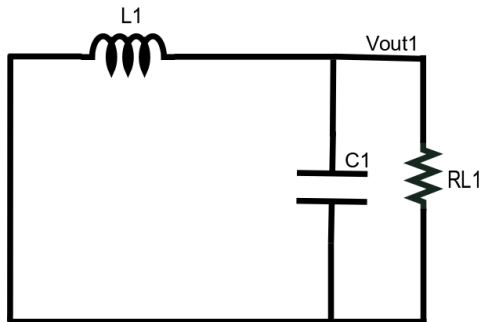


Figure 2.6: The buck converter circuit during OFF-state

The advantages of buck converter are high efficiency, less expensive. The general equations for buck converters can be clarified as

$$L \frac{di_{L1}}{dt} = qV_{in1} - v_{out1}, \quad (2.13)$$

$$C_1 \frac{dv_{out1}}{dt} = i_{L1} - \frac{V_{out1}}{R_{L1}}, \quad (2.14)$$

2.2 Detailed Model of Switching Converter

The detailed model (DET) is considered one of the fundamental models that describes average behavior and estimate the ripple behaviors in the converter. The DET model attempts to illustrate the actual detailed behavior of each switch. This converter has been used the pulse width modulation technique to control the switch in this circuit by using continuous condition mode with switching function

and duty cycle as shown in Fig.2.7 [12, 13]. The equations 2.15 and 2.16 illustrate the DET model in boost converter.

$$L \frac{di_{L2}}{dt} = V_{in2} - (1 - q)V_{out2}, \quad (2.15)$$

$$C \frac{dv_{out2}}{dt} = (1 - q)i_{L2} - i_{out2}, \quad (2.16)$$

The q is the switching function as shown in Fig.2.7 . If the transistor is ON, the q will be 1, but if it is OFF, the q will be 0. The general differential equation is built to portray the detailed model of the boost converter when the transistor is ON-OFF

$$\dot{x} = q(A_1x + B_1u) + (1 - q)(A_2x + B_2u), \quad (2.17)$$

where A_1 and A_2 are matrices, x is the state variables vector, u is the input vector, and B_1 and B_2 are input matrices [12, 14]

$$x = \begin{bmatrix} i_{L2} \\ v_{out2} \end{bmatrix}, u = V_{in}, A_1 = \begin{bmatrix} 0 & 0 \\ 0 & -\frac{1}{R_{L2}C_2} \end{bmatrix}, A_2 = \begin{bmatrix} 0 & -\frac{1}{L} \\ \frac{1}{C_2} & -\frac{1}{R_{L2}C_2} \end{bmatrix}, B_1 = B_2 = \begin{bmatrix} \frac{1}{L} \\ 0 \end{bmatrix}, \quad (2.18)$$

Equations 2.19 and 2.20 for the detailed model are specified during the switches ON and OFF in buck converters. The detailed model for the buck converter is described as

$$L \frac{di_{L1}}{dt} = qV_{in1} - V_{out1}, \quad (2.19)$$

$$C_1 \frac{dv_{out1}}{dt} = i_{L1} - i_{out1}, \quad (2.20)$$

$$i_{out1} = \frac{v_{out1}}{R_{L1}}, \quad (2.21)$$

The DET model has a long run time simulation compared to other models and does not have a constant equilibrium because the state variables waveforms are produced from DET model in this converter always oscillate and never go to steady state. 2.22 is combined with the equations above to illustrate when the transistor is ON-OFF in the buck converter.

$$\dot{x} = q(A_1x + B_1u) + (1 - q)(A_2x + B_2u), \quad (2.22)$$

where

$$x = \begin{bmatrix} i_{L1} \\ v_{out1} \end{bmatrix}, u = V_{in}, A_1 = A_2 = \begin{bmatrix} 0 & -\frac{1}{L} \\ \frac{1}{C} & -\frac{1}{R_{L1}C_1} \end{bmatrix}, B_1 = \begin{bmatrix} \frac{1}{L} \\ 0 \end{bmatrix}, B_2 = \begin{bmatrix} 0 \\ 0 \end{bmatrix}, \quad (2.23)$$

2.3 State Space Average Model

The state space averaging (SSA) technique has been constructed in dc-dc converters to analyze the average behavior in the converters. The standard forms for SSA model are given below:

$$\dot{x} = \bar{A}x + \bar{B}u \quad (2.24)$$

$$y = \bar{C}x + \bar{D}u \quad (2.25)$$

where \bar{A} , \bar{B} , \bar{C} , and \bar{D} are the system matrices, \dot{x} is the derivative of state variable, u is the input signal, and y is the vector output signal. The SSA model has been used the duty cycle (D) in the dc-dc converters. The state space model has been implemented in boost converter. When the transistor is ON, as mentioned earlier, $DT_s w$ ($T_s w$ is the switching cycle), the input voltage (V_{in2}) charge the inductor as described in 2.26. The inductance current does not flow through the capacitor and load, therefore, both of them are isolated from the circuit as defined in 2.27 [15, 16].

$$L \frac{di_{L2}}{dt} = V_{in2} \quad (2.26)$$

$$0 = C_2 \frac{dv_{out2}}{dt} + \frac{v_{out2}}{R_{L2}} \quad (2.27)$$

where i_{L2} is the inductance current, V_{in2} is the input voltage, C_2 is the capacitor value, v_{out2} is the capacitor voltage, and R_{L2} is the load resistance in boost converter. The equation 2.28 describes state space averaging model in boost converter during ON state.

$$\begin{bmatrix} \frac{di_{L2}}{dt} \\ \frac{dv_{out2}}{dt} \end{bmatrix} = \begin{bmatrix} 0 & 0 \\ 0 & -\frac{1}{R_{L2}C_2} \end{bmatrix} \begin{bmatrix} i_{L2} \\ v_{out2} \end{bmatrix} + \begin{bmatrix} \frac{1}{L} \\ 0 \end{bmatrix} V_{in2} \quad (2.28)$$

where $A_{1s(ON)} = \begin{bmatrix} 0 & 0 \\ 0 & -\frac{1}{R_{L2}C_2} \end{bmatrix}$ and $B_{1s(ON)} = \begin{bmatrix} \frac{1}{L} \\ 0 \end{bmatrix}$ are the matrices in the boost converter. The duty cycle is taken as switching function (D), during OFF time $(1-D)T_s$, the transistor is OFF, and the diode is ON. The inductor current will flow through the capacitor and resistor as illustrated below. The equations 2.29 and 2.30 described during OFF time

$$L \frac{di_{L2}}{dt} = V_{in2} - v_{out2} \quad (2.29)$$

$$C_2 \frac{dv_{out2}}{dt} = i_{L2} - \frac{v_{out2}}{R_{L2}} \quad (2.30)$$

The state space averaging equation of boost converter during OFF state is illustrated as

$$\begin{bmatrix} \frac{di_{L2}}{dt} \\ \frac{dv_{out2}}{dt} \end{bmatrix} = \begin{bmatrix} 0 & \frac{1}{L} \\ \frac{1}{C_2} & -\frac{1}{R_{L2}C_2} \end{bmatrix} \begin{bmatrix} i_{L2} \\ v_{out2} \end{bmatrix} + \begin{bmatrix} \frac{1}{L} \\ 0 \end{bmatrix} u, \quad (2.31)$$

$$\text{where } A_{1s(OFF)} = \begin{bmatrix} 0 & \frac{1}{L} \\ \frac{1}{C_2} & -\frac{1}{R_{L2}C_2} \end{bmatrix} \text{ and } B_{2s(OFF)} = \begin{bmatrix} \frac{1}{L} \\ 0 \end{bmatrix}.$$

To obtain the general state space equation, the average of \bar{A} and \bar{B} matrices have been derived with the switching duty cycle as defined

$$\dot{x}_0 = (A_{1s(ON)}D + A_{1s(OFF)}(1-D))x_0 + (B_{1s(ON)}D + B_{2s(OFF)}(1-D))u \quad (2.32)$$

$$\bar{A} = (A_{1s(ON)}D + A_{1s(OFF)}(1-D)) \quad (2.33)$$

$$\bar{B} = (B_{1s(ON)}D + B_{2s(OFF)}(1-D)) \quad (2.34)$$

The general state space equation for boost converter is illustrated in equation 2.35.

$$\begin{bmatrix} \frac{di_L}{dt} \\ \frac{dv_{out}}{dt} \end{bmatrix} = \begin{bmatrix} 0 & -\frac{(1-D)}{L} \\ \frac{(1-D)}{C_2} & -\frac{1}{C_2R_{L2}} \end{bmatrix} \begin{bmatrix} i_{L2} \\ v_{out2} \end{bmatrix} + \begin{bmatrix} \frac{1}{L} \\ 0 \end{bmatrix} u, \quad (2.35)$$

Likewise, the state space model has been implemented in buck converter. Fig. 2.4 shows the buck converter when the transistor is ON.

$$v_{out2} = V_{in2} - L \frac{di_{L2}}{dt} \quad (2.36)$$

$$i_L = C_2 \frac{dv_{out2}}{dt} + \frac{v_{out2}}{R_{L2}} \quad (2.37)$$

The state space equation for buck converter during ON state is formulated

$$\begin{bmatrix} \frac{di_L}{dt} \\ \frac{dv_{out}}{dt} \end{bmatrix} = \begin{bmatrix} 0 & -\frac{1}{L} \\ \frac{1}{C_2} & -\frac{1}{C_2 R_{L2}} \end{bmatrix} \begin{bmatrix} i_{L2} \\ v_{out2} \end{bmatrix} + \begin{bmatrix} \frac{1}{L} \\ 0 \end{bmatrix} u, \quad (2.38)$$

where $A_{1sb(ON)} = \begin{bmatrix} 0 & -\frac{1}{L} \\ \frac{1}{C_2} & -\frac{1}{C_2 R_{L2}} \end{bmatrix}$, $B_{1sb(ON)} = \begin{bmatrix} \frac{1}{L} \\ 0 \end{bmatrix}$.

Otherwise, During OFF state, the transistor is OFF, and the state space equation is derived below

$$\begin{bmatrix} \frac{di_L}{dt} \\ \frac{dv_{out}}{dt} \end{bmatrix} = \begin{bmatrix} 0 & -\frac{1}{L} \\ \frac{1}{C_2} & -\frac{1}{C_2 R_{L2}} \end{bmatrix} \begin{bmatrix} i_L \\ v_{out} \end{bmatrix} + \begin{bmatrix} 0 \\ 0 \end{bmatrix} u, \quad (2.39)$$

where $A_{2sb(OFF)} = \begin{bmatrix} 0 & -\frac{1}{L} \\ \frac{1}{C_2} & -\frac{1}{C_2 R_{L2}} \end{bmatrix}$, $B_{2sb(OFF)} = \begin{bmatrix} 0 \\ 0 \end{bmatrix}$,

The equivalent state space equation for the buck converter during ON-OFF state is calculated below:

$$\bar{A} = A_{1sb(ON)}D + A_{2sb(OFF)}(1 - D) \quad (2.40)$$

$$\bar{B} = B_{1sb(ON)}D + B_{2sb(OFF)}(1 - D) \quad (2.41)$$

$$\begin{bmatrix} \frac{di_L}{dt} \\ \frac{dv_{out}}{dt} \end{bmatrix} = \begin{bmatrix} 0 & -\frac{1}{L} \\ \frac{1}{C_2} & -\frac{1}{C_2 R_{L2}} \end{bmatrix} \begin{bmatrix} i_L \\ v_{out} \end{bmatrix} + \begin{bmatrix} \frac{D}{L} \\ 0 \end{bmatrix} u, \quad (2.42)$$

where $\bar{A} = \begin{bmatrix} 0 & -\frac{1}{L} \\ \frac{1}{C} & -\frac{1}{RC} \end{bmatrix}$ and $\bar{B} = \begin{bmatrix} \frac{D}{L} \\ 0 \end{bmatrix}$

in [17], the paper is used the SSA technique to get the dynamic and the steady-state model for a hybrid switched-capacitor boost converter. In [18], this paper is addressed the SSA model of PWM converters in continuous and discontinuous modes. In this approach, the duty cycle ratio constraint and the correction term are taken numerically by using the DET simulation. The accuracy of the averaged model has been proved in time-domain and frequency-domain. In [19, 20], these paper were presented the SSA model for boost and buck switching regulators and employed to design an accurate controller that has stability states. The non-ideal

impacts in dc-dc converters, such as capacitance resistor and inductor resistor, are counted in this paper. This model was also simulated in both PSpice and compared its results with MATLAB program and the results are approximately identical.

2.4 Generalized Average Method

The generalized average method (GAM) is the model that used for analyzing and predicting the ripple in power systems by using the software program such as Simulink . In this work, the GAM is used in dc-dc converter to estimate the ripple and average behaviors in these converters. This method has a stability issue that is explained more in this section. The GAM is simulated in boost and buck converters in Simulink program and it does not take a long simulation run time compared to detailed model. This model works more precisely than the SSA model because it can predict the ripple behavior in the converters variables, but the SSA does not. The GAM was used the pulse width modulation technique as switching function used a finite Fourier series to represent dc fundamental and harmonics behavior for the result of converters variables [21–25].

2.5 Definition of Fourier Series

The $x(t)$ can be considered as the state variable in the dc-dc converter. The state variables are the i_L and v_{out} signals from boost and buck converter circuits. The GAM is able to estimate the dc fundamental and harmonics by using Fourier series. The Fourier series equation is written

$$x(t) \approx x_0(t) + \sum_{n=1}^N \left(x_{nc}(t) \cos \frac{2\pi t}{T} + x_{ns}(t) \sin \frac{2\pi t}{T} \right) \quad (2.43)$$

$x_0(t), x_{nc}(t), x_{ns}(t)$ are the real-valued trigonometric Fourier series variables, and the $\frac{2\pi t}{T}$ is the angle of switching function. These terms can be used for the dc fundamental, the harmonics results, and the switching ripple in the dc-dc con-

verters. The subscripts c and s refer to the cosine and sine coefficients. N is the number of the series term that represents the harmonics for the variables state. Equation 2.43 generates $(2N + 1)$ variables. If the N value is one or two, it will be enough to determine the switching ripples and more accurate than $N = 0$ [26, 27].

The vector can be extracted from equation 2.43 as described

$$X = [x_0 \ x_{1c} \ x_{1s} \ \dots \ x_{Nc} \ x_{Ns}]^T \quad (2.44)$$

The vector X is used to rewrite equation 2.43 as defined

$$x(t) = s(t)X \quad (2.45)$$

where $s(t)$ is defined as

$$s(t) = \left[1 \ \cos\frac{2\pi}{T}t \ \sin\frac{2\pi}{T}t \ \dots \ \cos N\frac{2\pi}{T}t \ \sin N\frac{2\pi}{T}t \right] \quad (2.46)$$

As shown below, $x(t)$ was substituted into the inductor current ($i_L(t)$), capacitor voltage ($v_{out}(t)$), and switch function $q(t)$ in equations 2.47 2.48, 2.49, respectively [25].

$$i_L(t) \approx i_{L0} + i_{L1c} \cos(\omega t) + i_{L1s} \sin(\omega t) \quad (2.47)$$

$$v_{out}(t) \approx v_{out0} \cos(\omega t) + v_{out1s} \sin(\omega t) \quad (2.48)$$

$$q(t) \approx q_0 + q_{1c} \cos(\omega t) + q_{1s} \sin(\omega t) \quad (2.49)$$

2.6 The Time Derivative of Fourier Series Waveform

Since the waveform $x(t)$ changes with time, the $x(t)$ in equation 2.43 has been derived with time in Nth-order in equation 2.50 and this derivative is part of GAM method. The average vector in the GAM method can represent as described [25, 28, 29]

$$\begin{aligned} \frac{dx(t)}{dt} = & \left\{ \frac{dx_0}{dt} + \sum_{n=1}^N \left(\frac{2n\pi}{T} \right) x_{ns} \cos\left(\frac{2n\pi}{T}t\right) - \left(\frac{2n\pi}{T} \right) x_{nc} \sin\left(\frac{2n\pi}{T}t\right) \right. \\ & \left. + \sum_{n=1}^N \left(\frac{dx_{nc}}{dt} \right) x_{ks} \cos\left(\frac{2n\pi}{T}t\right) + \left(\frac{dx_{ns}}{dt} \right) \sin\left(\frac{2n\pi}{T}t\right) \right\} \end{aligned} \quad (2.50)$$

The equation 2.6 has been differentiated with respect the time as defined

$$\frac{dx(t)}{dt} = \frac{d}{dt}(s(t)X) \quad (2.51)$$

$$= \frac{ds(t)}{dt}X + s(t)\frac{dX}{dt} \quad (2.52)$$

$$\frac{dx(t)}{dt} = s(t)\left(AX + \frac{dX}{dt}\right) \quad (2.53)$$

$\frac{dX}{dt}$ is the derivative of the average vector, and A represents the matrix $(2K + 1) \times (2K + 1)$. The matrix values are zero everywhere

except $A_{(2k,2k+1)} = k\omega$, $A_{(2k+1,2k)} = -k\omega$, and $k \in \{1, 2, \dots, K\}$. The analysis from the output dc-dc converters can be calculated into equation 2.47 or 2.48 as shown below

$$\frac{dx_0}{dt} = \frac{dx_0}{dt} \quad (2.54)$$

$$\frac{dx_{1c}}{dt} = \frac{dx_c}{dt} + k\omega x_{ns} \quad (2.55)$$

$$\frac{dx_{1s}}{dt} = \frac{dx_{ks}}{dt} - k\omega x_{nc} \quad (2.56)$$

The equations above can be represented by an average vector with a *Nth*-series.

2.7 Product Average Signals in DC-DC Converter

A switching function and voltage or current output signal should be multiplied using discrete convolution method. For instance, assuming $x(t)$ represents the capacitor voltage signal and $y(t)$ represents the switching function, and both are approximated by *Nth*-

order series then the product of the averages of these terms as shown below [30, 31]

$$z(t) = x(t)y(t) = z_0(t) + \sum_{n=1}^N \left(z_{nc}(t) \cos\left(n\frac{2\pi t}{T}\right) + z_{ns}(t) \sin\left(n\frac{2\pi t}{T}\right) \right) \quad (2.57)$$

The $z(t)$ equation can be reconstructed as

$$z(t) = (s(t)X)(s(t)Y) \quad (2.58)$$

The multiplication and implementation specification are achieved by using MATLAB program. The index-n terms are:

$$z_0 = x_0y_0 + \sum_{n=1}^N \left(\frac{x_{nc}y_{nc}}{2} + \frac{x_{nc}y_{nc}}{2} \right) \quad (2.59)$$

$$z_{nc} = x_0y_{nc} + x_{nc}y_0 \quad (2.60)$$

$$z_{ns} = x_0y_{ns} + x_{ns}y_0 \quad (2.61)$$

By using discrete convolution, the average z can be represented

as

$$z = \Omega(x)y \quad (2.62)$$

As clarified above, $\Omega(x)$ can be defined as

$$\Omega(x) = \begin{bmatrix} x_0 & \frac{1}{2}x_{1c} & \frac{1}{2}x_{1s} \\ x_{1c} & x_0 & 0 \\ x_{1s} & 0 & x_0 \end{bmatrix} \quad (2.63)$$

This matrix $(2K + 1) \times (2K + 1)$ is used in the product subsystem when the state variables, that is produced from buck and boost converters, multiply with the switching function. The $\Omega(x)$ can be substituted with q and y can be substituted with voltage or current. For instance, equation 2.7 is clarified the multiplication between the switching function $q(t)$ and state variables (capacitor voltage (v_{out})) in the boost converter.

$$(1 - q)v_{out} \rightarrow \begin{bmatrix} 1 - q_0 & -\frac{1}{2}q_{1c} & -\frac{1}{2}q_{1s} \\ -q_{1c} & 1 - q_0 & 0 \\ -q_{1s} & 0 & 1 - q_0 \end{bmatrix} \begin{bmatrix} v_{out0} \\ v_{out1c} \\ v_{out1s} \end{bmatrix} \quad (2.64)$$

$$\begin{aligned}
&= (1 - q_0)v_{out0} - \frac{1}{2}q_{1c}v_{out1c} - \frac{1}{2}q_{1s}v_{out1s} - q_{1c}v_{out0} - (1 - q_0)v_{out1c} - \\
&\quad q_{1s}v_{out0} + (1 - q_0)v_{out1s}
\end{aligned} \tag{2.65}$$

2.8 The Switching Function of DC-DC converter

In dc-dc converters, the diode and transistor work as a switching function. The q , can control the system and the duty cycle compares with the carrier function (sawtooth waveform). If the D is larger than carrier function, the q will be one if it is less than sawtooth waveform, the q will be zero as shown in Fig. 3.1. The Fourier series coefficient of q are given for the switching function

$$q_0 = D, \tag{2.66}$$

$$q_{nc} = \frac{1}{n\pi} \sin(2n\pi D), \tag{2.67}$$

$$q_{ns} = \frac{1}{\pi} (1 - \cos(2n\pi D)), \tag{2.68}$$

The q_0, q_{nc}, q_{ns} are the index-0, index-nc, and index-ns averages, respectively. These are constant for the open loop circuit when D is constant [29, 32].

2.9 GAM Model of the DC-DC converters

2.9.1 The GAM Model of the Boost Converter

The GAM model has been built in the boost converter as shown in Fig. 2.3. This boost converter is operating in continuous conduction mode. By using the GAM model in the boost converter, the state variable is defined as

$$V_{in2} - (1 - q)v_{vout2} = L \left(Ai_{L2} + \frac{di_{L2}}{dt} \right) \quad (2.69)$$

$$C2 \left(Ai_{L2} + \frac{di_{L2}}{dt} \right) = (1 - q)i_{L2} - \frac{v_{out2}}{R_{L2}} \quad (2.70)$$

where q is the switching function that represents the transistor condition. These equations are constructed in Simulink, and the results will be explained in chapter 4.

2.9.2 Using the GAM Model in the Buck Converter

The GAM has been used in the ideal buck converter circuit as shown in 2.3. In this model, the buck converter is also operating in continuous conduction mode. The state variables of the buck converter in GAM model are given.

$$qV_{in1} - v_{out1} = L \left(Ai_{L1} + \frac{di_{L1}}{dt} \right) \quad (2.71)$$

$$i_{L1} - \frac{v_{out}}{R_{L1}} = C1 \left(Av_{out1} + \frac{dv_{out1}}{dt} \right) \quad (2.72)$$

where q is the switching function that represents the transistor condition. These equations are constructed in Simulink, and the results will be explained in chapter 4. In [33], the proposed model for dc-dc converters depends on mathematical methods for periodic differential equations are approximately similar to the GAM model because it predicated the average ripple behavior in dc-dc converters. This model used the multi-frequency to approximate the average behavior and also correct the dc offset error that happened in the conventional method on closed-loop circuit. In [34] the general-

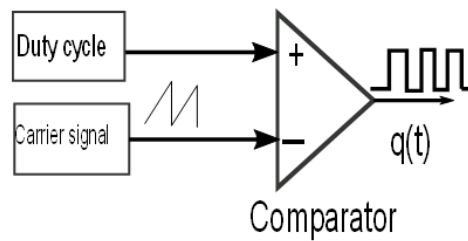
ized state-space averaging method (GSSA) presented for modeling multi-converters dc. The GSSA was able to estimate the average of state variable, and ripple behavior.

2.10 Pulse Width Modulation in Power Electronics

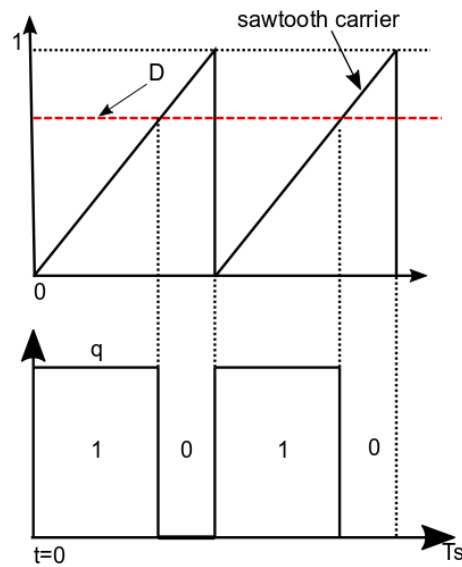
The modulation is the method that changes some characteristics of a periodic waveform, named the carrier signal. The modulation signal has the information to be transferred. PWM controller is widely used in industry dc-dc converters because the PWM is able to improve the power efficiency in dc-dc converters. This method is also employed for speed controller and is widely used in devices such as fans. The PWM can adjust the signal between the 1 or 0 and can control the power and speed the device. As mentioned earlier, the PWM has been used in DET and GAM models. The PWM signal is generated using an analog signal sawtooth carrier that increases from 0 volt to 1 volt and comparing it to a duty cycle D . If the D is above the carrier sawtooth, $q(t)$ will be 1 and if the D is less than the carrier sawtooth, q will be 0. by changing D , the PWM will

be affected. Fig. 2.4 shows the relationship among the PWM carrier $c(t)$, the duty cycle $d(t)$, and the switching function q in detailed model. The buck converter averages the PWM signal, charging the inductor and capacitor when the transistor is ON and keeping the signal stable when the transistor is OFF. The boost converter essentially charges up the inductor for the time that the transistor ON and sends the current to charge the capacitor when the transistor is OFF. In [35], PWM is used to delete some lower-order harmonic and attempts to obtain developed performance in output signal such reducing the ripple and torque in single-phase and three-phase inverters. Also, in this paper, programmed PWM and conventional PWM is compared. In [36], the PWM dc-dc converters has been controlled in two types of three-phase resonant. PWM control technique was able to reduce the losses switching while managing the output voltage from no load to full load. In ref [37, 38], the paper presented the theory of PWM in dc-dc converters to describe the dynamic behavior for boost, buck, buck-boost, and cuk converters and to assist built a system with improved results. In [39], two PWM gating methods

(APWM and TEPWM) employed for improving the efficiency of the converter. These techniques are also compared with PSM technique and approved that APWM and TEPWM method have better characteristics than the PSM.



(a)



(b)

Figure 2.7: Pulse width modulation

2.11 Stability in Power Electronics

Because of the stability property in power electronics, the power system is able to return to the steady state condition after submitting to the disturbance. The example of the disturbance is short circuit between the line and the earth, variations in load. Stability analysis is widely used in ships, airplane, and spacecraft. There are several methods that approve the stability in the power electronics such as Lyapunov, Fliest, and La Salle's invariance theory. In this work, the Lyapunov theory has been used to approve the stability of new model. In [40] Lyapunov stability theory used to investigate that is dc-dc boost is marginally stable. In [41], the linearization method has been applied to stabilize the output voltage of the dc-dc converters. In [42] the genetic algorithm has been constructed in converters for predicate the regions of stability. Also, this paper employed different Lyapunov functions to assign the regions of stability. In [43], Lyapunov function technique was employed to analyze the stability and control design in switched system.

Chapter 3

Stabilized Generalized Averaging Model in DC-DC Converters

3.1 Stabilized Generalized Averaging Model (SGAM)

The proposed SGAM is a useful model for analysis and design the power electronic systems. This model can estimate the average behavior and the ripple behavior of the dc-dc converters. The method is simple, does not have restrictions, and faster than DET model, and can use multi-converters. The integrator of SGAM was constructed. The SGAM integrator consists of two new matrices that connected inside the subsystem in Simulink. The stabilized GAM model has been proposed for a dc-dc converter. The waveform $x(t)$ signal from the SGAM can be analyzed by using a Fourier series in

the dc-dc converter. As discussed earlier. The rest of this chapter is organized as follows. The Integrator of SGAM in Section (3.2) The SGAM model of a buck and a boost converter is described in Sections (3.3). Also, in Section (3.4), a stability in SGAM models is explored. The contribution work: 1) A SGAM method has been used sampled PWM converters. 2) A solution to the observed stability problem is observed and described.

3.2 Using Fourier Series in SGAM

As mentioned in the GAM model, the SGAM is used the Fourier series, $x(t)_1$, to analyze the state variables converters. The state variables are the i_{sL} and v_{sout} signals from boost and buck converters circuits. These signals have dc value and harmonics. A Fourier series can be analyzed the state variables and can determined the dc value and harmonics. The Fourier series equation below has terms

that can represent the output of dc-dc converters.

$$x(t)_1 \approx x_{s0}(t) + \sum_{n=1}^N \left(x_{snc}(t) \cos \frac{2n\pi t}{T} + x_{sns}(t) \sin \frac{2n\pi t}{T} \right) \quad (3.1)$$

$x_{s0}(t), x_{snc}(t), x_{sns}$ are the real-valued trigonometric Fourier series coefficients. These terms can be used for the dc fundamental, the harmonics results, and switching ripple in the dc-dc converters.

N is the number of the terms in the series that represent the harmonics for the variables state. If the N value is one or two, it will be sufficient to determine the harmonics. The vector of length $(2N + 1)$ can be extracted from equation 3.1 as described

$$X_s = [x_{s0} \ x_{s1c} \ x_{s1s}, \dots, x_{sNc} \ x_{sNs}]^T. \quad (3.2)$$

The vector X_s is used to rewrite equation 3.1 as defined

$$x(t)_1 s(t)_s X_s \quad (3.3)$$

where $s(t)_{sis}$ defined as

$$s(t)_s = [1 \cos(N\frac{2\pi}{T})t, \sin(N\frac{2\pi}{T})t \dots \cos(N\frac{2\pi}{T})t, \sin(N\frac{2\pi}{T})t]. \quad (3.4)$$

As shown below, $x(t)_1$ was substituted into the inductor current $i_{sL}(t)$, capacitor voltage $v_{sout}(t)$, and switch function $q(t)$ in 3.5, 3.6 and 3.7, respectively

$$i_{sL}(t) \approx i_{sL0} + i_{sL1c} \cos(\omega t) + i_{sL1s} \sin(\omega t) \quad (3.5)$$

$$v_{sout}(t) \approx v_{sout0} \cos(\omega t) + v_{sout1s} \sin(\omega t) \quad (3.6)$$

$$q(t)_s \approx q_{s0} + q_{s1c} \cos(\omega t) + q_{s1s} \sin(\omega t) \quad (3.7)$$

3.3 Product Average Signals in DC-DC Converter

A switching function and voltage or current output signal should be multiplied by using discrete convolution method. For instance,

$x(t)$ represents the capacitor voltage or inductor current signal and $y(t)$ represents the switching function, and both are approximated by N th-order series. The product of the averages of these terms is illustrated [30, 31]

$$\langle x(t).y(t) \rangle = \sum_{i=-\infty}^{\infty} \langle x(t) \rangle_{n-i} \langle y(t) \rangle_i \quad (3.8)$$

By using discrete convolution to calculate the index-N average of a product term such as $(1 - q)V_{out}$, the term is described as

$$(1 - q)V_{out} \Rightarrow \begin{bmatrix} 1 - q_0 & -\frac{1}{2}q_{1c} & -\frac{1}{2}q_{1s} \\ q_{1c} & 1 - q_0 & 0 \\ -q_{1s} & 0 & 1 - q_0 \end{bmatrix} \begin{bmatrix} V_{out0} \\ V_{out1c} \\ V_{out1s} \end{bmatrix} \quad (3.9)$$

$$\begin{aligned} &= (1 - q_0)V_{out0} - \frac{1}{2}q_{1c}V_{out1c} - \frac{1}{2}q_{1s}V_{out1s} - q_{1c}V_{out0} \\ &\quad - (1 - q_0)V_{out1c} - q_{1s}V_{out0} + (1 - q_0)V_{out1s} \end{aligned} \quad (3.10)$$

3.3.1 The Switching Function of Dc-Dc Converter

In the dc-dc converters, the diode and transistor work as a switch, and this switching function, q , can control the system. When the

switch is ON or OFF, it will represent 1 or 0 in the converters, respectively. Then, the converters will use duty ratio, D , in the average of the switching function, and the D will be a constant value. The Fourier series terms are given when the switching is ON.

$$q_0 = D, \quad (3.11)$$

$$q_{nc} = \frac{1}{\pi}(\sin(2n\pi D)),, \quad (3.12)$$

$$q_{ns} = \frac{1}{\pi}(1 - \cos(2n\pi D)), \quad (3.13)$$

The q_0 , q_{nc} , q_{ns} are the *index – 0*, *index – nc*, and *index – ns*, respectively, average at duty cycle D [14].

3.4 The Integrator of the Stabilized Generalized Averaging Model

A SGAM is a system of differential equations that was built in dc-dc converters and this method attempt to stabilize the behavior

in GAM . This technique is a powerful method to analysis the dc-dc converter behavior and is easy to apply. The harmonics and fundamental dc signals that results from boost and buck converters are examined by using the Fourier series theory. The equation 3.4 has been derivative with respect the time as defined

$$\frac{dx(t)_1}{dt} = \frac{d}{dt}(s(t)_s X_s) \quad (3.14)$$

$$= \frac{ds(t)_s}{dt} X_s + s(t)_s \frac{dX_s}{dt} \quad (3.15)$$

$$= s(t)_s (T_2 \frac{dX_s}{dt} + S_2 X_s) \quad (3.16)$$

$\frac{dX_s}{dt}$ is the derivative of the average vector, S_2 and T_2 represent the matrices $(2N + 1) \times (2N + 1)$.

where S_2 and T_2 are matrices that assist to stabilize the system

and $n \in \{1, 2, \dots, N\}$

$$S_2 = \begin{bmatrix} 0 & \frac{\alpha}{2}\cos\theta & \frac{\alpha}{2}\sin\theta \\ 0 & -\frac{\alpha}{2} & -\omega \\ 0 & \omega & \frac{-\alpha}{2} \end{bmatrix}, T_2 = \begin{bmatrix} 1 & \frac{-\alpha}{2\omega}\sin\theta & \frac{\alpha}{2}\cos\theta \\ 0 & 1 & \frac{-\alpha}{2\omega} \\ 0 & \frac{\alpha}{2\omega} & 1 \end{bmatrix} \quad (3.17)$$

$\alpha, \theta,$ and ω are constants that are in the matrices. These matrices are built it inside the subsystem to make the SGAM integrator and used to stabilize the approach.

3.5 Using Stabilized Generalized Averaging Model in DC-DC Converter

3.5.1 The SGAM of Boost Converter

The proposed SGAM has been applied in the boost converter as shown in Fig.2.1. Also, the sections 3.5.1 and 3.5.2 can be used in the SGAM. The inductor current and capacitor voltage equations are given

$$L(S_2 i_{sL} + T_2 \frac{di_{sL}}{dt}) = V_{in2} - (1 - q)v_{sout} \quad (3.18)$$

[The $\frac{di_{sL}}{dt}$ is consist of $\frac{di_{sL0}}{dt}$, $\frac{di_{sL1c}}{dt}$, $\frac{di_{sL1s}}{dt}$]

$$C2\left(S_2v_{sout} + T_2\frac{dv_{sout}}{dt}\right) = (1 - q)i_{sL} - \frac{v_{sout}}{R_{L2}} \quad (3.19)$$

[The $\frac{dv_{sout}}{dt}$ is consist of $\frac{dv_{sout0}}{dt}$, $\frac{dv_{sout1c}}{dt}$, $\frac{dv_{sout1s}}{dt}$]

3.5.2 The SGAM of Buck Converter

The proposed SGAM has been used in the ideal buck converter circuit as shown in Fig. 2.3. In this model, the buck converter is operating in continuous conduction mode. The sections 3.5.1 and 3.5.2 can be used in the SGAM. The state variables for SGAM (inductor current and capacitor voltage equations) are given.

$$V_{in1}q - v_{sout} = L\left(S_2i_{sL} + T_2\frac{di_{sL}}{dt}\right) \quad (3.20)$$

$$i_{sL} - \frac{v_{sout}}{R_{L1}} = C2\left(S_2v_{sout} + T_2\frac{dv_{sout}}{dt}\right) \quad (3.21)$$

where q is the switching function that represents the transistor condition. These equations are constructed in Simulink, and the results will be explained in chapter 4.

3.6 Transformation to Constant Matrix (P)

To prove the stability the integrator

$$\dot{x} = S_2x + T_2u \quad (3.22)$$

Let $z = Px$ where $P = \begin{bmatrix} 1 & \cos\theta & \sin\theta \\ 0 & 1 & 0 \\ 0 & 0 & 1 \end{bmatrix}$

By differentiation z with respect time

$$\frac{dz}{dt} = \omega \frac{dP}{d\theta} x + P(S_2x + T_2u) \quad (3.23)$$

$$\frac{dz}{dt} = \left(\omega \frac{dP}{d\theta} P^{-1} + PS_2P^{-1} \right) z + PT_2u \quad (3.24)$$

By substituting P , $\frac{dP}{d\theta}$, T_2 , and S_2 into equation 3.6

$$\frac{dz}{dt} = \begin{bmatrix} 0 & 0 & 0 \\ 0 & -\frac{\alpha}{2} & -\omega \\ 0 & \omega & -\frac{\alpha}{2} \end{bmatrix} z + \begin{bmatrix} 1 & \cos\theta & \sin\theta \\ 0 & 1 & -\frac{\alpha}{2\omega} \\ 0 & \frac{\alpha}{2\omega} & 1 \end{bmatrix} u \quad (3.25)$$

The eigenvalues of first matrix

$$\lambda_1 = 0$$

$$\lambda_2 = -\frac{\alpha}{2} - j\omega$$

$$\lambda_3 = -\frac{\alpha}{2} + j\omega$$

The eigenvalues of second matrix

Suppose

$$\bar{z} = \bar{P}\bar{x} \quad (3.26)$$

The differentiate \bar{z} respect with time

$$\dot{\bar{z}} = \omega \frac{d\bar{P}}{d\theta} \bar{P}^{-1} \bar{z} + \bar{P} (\bar{A} \bar{P}^{-1} \bar{z} + \bar{B} \bar{u}) \quad (3.27)$$

where

$$\bar{A} = I_N \otimes S_2 + A \otimes T \quad (3.28)$$

$$\bar{B} = B \otimes T \quad (3.29)$$

By simplify equation 3.6

$$\dot{\bar{z}} = \omega(I_N \otimes \frac{d\bar{P}}{d\theta})(I_N \otimes P^{-1})\bar{z} + (I_N \otimes P)(I_N \otimes S_2 + (A \otimes T)\bar{z} + \bar{B}\bar{u}) \quad (3.30)$$

Therefore,

$$= [I_N \otimes (\omega \frac{dP}{d\theta} P^{-1} + PS_2 P^{-1}) + A \otimes \begin{bmatrix} 1 & 0 & 0 \\ 0 & 1 & -\frac{\alpha}{2\omega} \\ 0 & \frac{\alpha}{2\omega} & 1 \end{bmatrix}] \bar{z} + (B \otimes T) \bar{u} \quad (3.31)$$

A and B are from SSA model (buck and boost converters)

3.7 The Stability in The SGAM integrator

Since the GAM has stability issue, the SGAM method has been presented below to approve the stability. Assume the SGAM integer has initial input value $u^{(i)} = [0 \ u_{1c}^i \ u_{1s}^i]$ where u_{1c}^i, u_{1s}^i are constants. The initial condition has taken in this integrator such as $X = [x_0 \ -\frac{u_{1s}^i}{\omega} \ -\frac{u_{1c}^i}{\omega}]$ where x_0 is zero, and $t = 0$, the input signal is changed $u^{(f)} = [0 \ u_{1c}^{(f)} \ u_{1s}^{(f)}]^T$, where $u_{1c}^{(f)} = u_{1c}^i$ when $u(t)$ is continuous. The

parameters of integrator are given in Table 3.1. The integrator of GAM equation in Chapter 2 in (GAM) is given below [44, 45]

Table 3.1: Integrator Parameter

ω	$1000\pi \text{ rad/s}$	x_0	0
$u_{1c}^{(i)}$	0.2	$u_{1c}^{(f)}$	0.2
$u_{1s}^{(i)}$	0.2	$u_{1s}^{(f)}$	0.3

Suppose an error variable is the discrepancy between the output value of the GAM model and SGAM model as illustrated $e(t) = y_2 - y_1$. If both integrator models have the same initial state $x_1(0) = x_2(0)$, the error should equal zero, and the error equation is derived below:

$$e(0) = s(t)(x_2(0) - x_1(0)) = 0 \quad (3.32)$$

The derivative $e(t)$ with respect time (the derivative is zero at all time because the $e(t)$ equal zero)

$$\frac{de}{dt} = \omega \frac{ds}{dt}(x_2 - x_1) + s(t) \left(\frac{dx_2}{dt} - \frac{dx_1}{dt} \right) \quad (3.33)$$

By substituting $\frac{ds}{d\theta}$, $s(t)$, $\frac{dx_2}{dt}$, and $\frac{dx_1}{dt}$ into equation above 3.7

where $\frac{dx_1}{dt}$ is average vector for GAM integrator,

$$\frac{dx_1}{dt} = s_1 x_1 + T_1 u, \quad (3.34)$$

$$\text{where } s_1 = \begin{bmatrix} 0 & 0 & 0 \\ 0 & 0 & -\omega \\ 0 & \omega & 0 \end{bmatrix}, T_1 = \begin{bmatrix} 1 & 0 & 0 \\ 0 & 1 & 0 \\ 0 & 0 & 1 \end{bmatrix}. \text{ see, reference [28]}$$

Therefore,

$$\begin{aligned} \frac{de}{dt} = \omega [0 \quad -\sin\theta \quad \cos\theta](x_2 - x_1) + [1 \quad \cos\theta \quad \sin\theta]s_1(x_2 - x_1) + \\ [1 \quad \cos\theta \quad \sin\theta](\Delta s x_2 + \Delta T u) \end{aligned} \quad (3.35)$$

Therefore

$$\begin{aligned} \frac{de}{dt} = [0 \quad -\omega \sin\theta \quad \omega \cos\theta] + \\ [0 \quad \omega \sin\theta \quad -\omega \cos\theta](x_2 - x_1) + s(t)(\Delta s x_2 + \Delta T u) \end{aligned} \quad (3.36)$$

The $e(t)$ and $\frac{de}{dt}$ are equal zero all time. The output SGAM model of integrator in time domain $x(t)$ matches to the output signal of GAM model integrator.

The integrators of DET, GAM, and SGAM has been compared in Simulink as shown in Fig. 3.1. The input for the DET integrator is unit step and the parameters for unit step are listed in Table 3.1. The time domain signals for DET, GAM, and SGAM are matched as shown in Fig. 3.3. The SGAM integrator is stable, and damping constant is the parameter that affects the stability system as shown Fig.3.2. However, the GAM integrator is unstable as shown in Fig. 3.4.

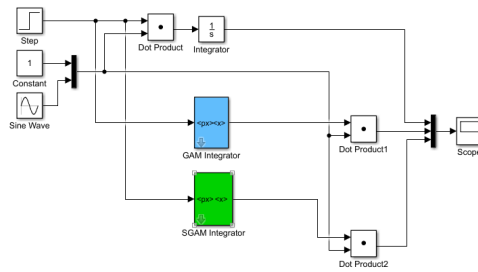


Figure 3.1: The comparison the integrator of DET, GAM, and SGAM models of integrator

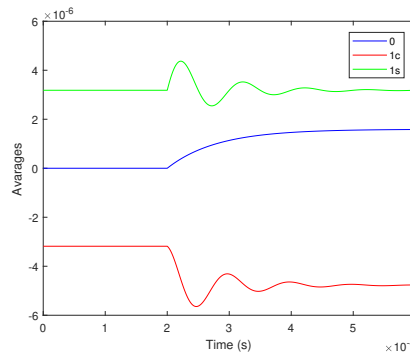


Figure 3.2: Shows the elements of x for SGAM model of integrator

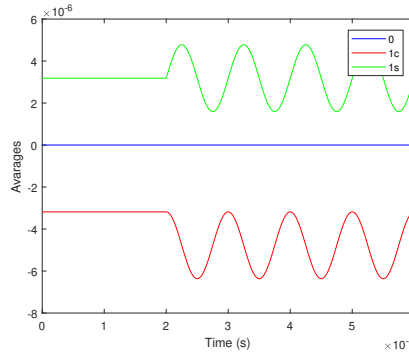


Figure 3.3: Shows the elements of x for SGAM model of integrator

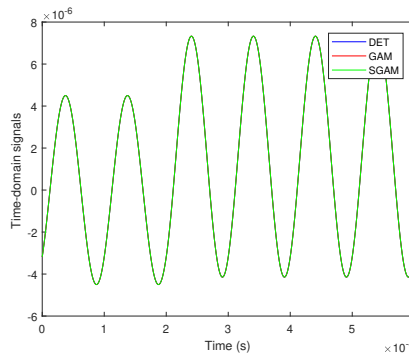


Figure 3.4: Time-domain signals of DET, GAM, and SGAM models of integrators

3.8 Lyapunov Function

In steady state, the $\frac{dx_1}{dt}$ equal zero in GAM model. The average vectors values in GAM integrator substitute into zero as below $\frac{dx_{1c}}{dt}$ and $\frac{dx_{1s}}{dt}$ equal zero (I mean derivative in equation (GAM) equal zero

in steady state).

$$\frac{dx_{1c}}{dt} = 0 = -\omega x_{1s} + u_{1c} \quad (3.37)$$

$$\frac{dx_{1s}}{dt} = 0 = \omega x_{1c} + u_{1s}. \quad (3.38)$$

The Lyapunov function has been used to predict the stability system. Assume $\frac{du_{1c}}{dt} = 0$ and $\frac{du_{1s}}{dt} = 0$ in the equation below

$$V = (-\omega x_{1s} + u_{1c})^2 + (-\omega x_{1c} + u_{1s})^2 \quad (3.39)$$

By derivative V , the results are given below

$$\frac{dV}{dt} = 2(-\omega x_{1s} + u_{1c})\left(-\omega \frac{dx_{1s}}{dt}\right) + 2(\omega x_{1c} + u_{1s})\left(\omega \frac{dx_{1c}}{dt}\right) \quad (3.40)$$

These values have been realized in steady-state and they substitute in the Lyapunov function equation to make the system stable end decay.

$$\delta_{1c} = \frac{-\alpha}{2\omega}(\omega x_{1c} + u_{1s}) \quad (3.41)$$

$$\delta_{1s} = \frac{\alpha}{2\omega}(-\omega x_{1s} + u_{1c}) \quad (3.42)$$

The time derivative of the Lyapunov function can be calculated as in equation 3.43

$$\frac{dV}{dt} = 2\omega(\omega x_{1s} + u_{1c})\delta_{1s} + 2\omega(\omega x_{1c} + u_{1s})\delta_{1c} = -\alpha V \quad (3.43)$$

The α value is an important parameter to make the system stable, and it might impact on the eigenvalue in the SGAM integrator.

3.9 Stability in DC-DC Converter

The results in Fig.3.2 and 3.4 show that the stabilized GAM model is stable with the additional poles created by the generalized averaging method assignable by parameter choice. The new GAM model predicts the same results as the existing GAM method without the underlying stability concerns. The stabilized GAM model exhibits constant equilibrium point and requires significantly lower run times than the DET model, but it is also able to predict the ripple performance of the converter. To prove the stability in the buck converter

in SGAM, the Kronecker product has been employed [46–48] as defined in equation 3.44

$$Abar = I_{n \times n} \otimes S_2 + A \otimes T_2, \quad (3.44)$$

where $I_{n \times n}$ is identity matrix, $A = \begin{bmatrix} 0 & -\frac{1}{L} \\ \frac{1}{C} & -\frac{1}{RC} \end{bmatrix}$ from the SSA model in buck converter, S_2 and T_2 are matrices that mentioned in section 3.2 . Since the eigenvalue of the $Abar$ is less than zero and the eigenvalues for the A are also less than zero, the SGAM is stable approach. By using the s-plane method in SGAM model [49–51], the all poles lie in the left- hand s- plane as illustrated in Fig. 3.5 and 3.6. The parameters in Table 3.1 are used in equation 3.44.

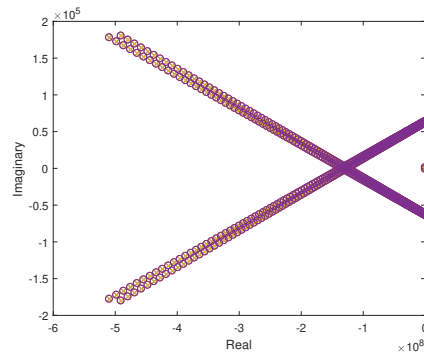


Figure 3.5: Shows the SGAM integrator model with various approximation orders in boost converter

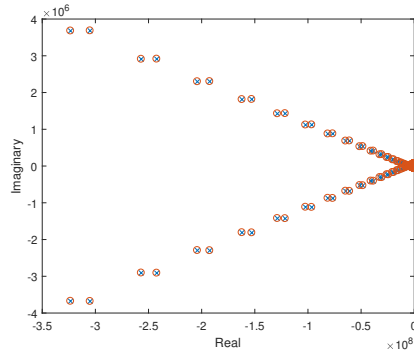


Figure 3.6: Shows the SGAM integrator model with various approximation orders in buck converter

Chapter 4

Simulation Results

4.1 Introduction

The SGAM model has been built in dc-dc converter in Simulink. The boost and buck converter have been used in this work, and The PWM signal has been applied in the buck and boost converters as shown in Fig. 2.7. The parameters have been used in Table 4.1 and 4.4, and the simulation for all models is constructed on personal computer (Intel(R) Core(TM) i5-4210U CPU @ 1.70 GHz, 8.00 GB RAM, 64-bit Operating System, x64-based processor). All models are constructed in ode23tb Simulink solver and the relative tolerance of 10^{-3} in MATLAB 2017a. Time tolerance is used $\text{equal}(10 * 128 * \text{eps})$, and the simulation time study for buck is 0.1 second and for boost is 0.4 second. All models such as DET, SSA,

GAM and SGAM are simulated and the results for all models are compared as clarified in this section. For the GAM and SGAM, the parameter α is taken approximately 10ω to make the integrator behavior stable. The simulation is taken when the mean run time equal 100 simulation. The run time simulation of DET, SSA, GAM and SGAM is illustrated in Table 4.3 and 4.2. The dc values and peak to peak (P-P) of capacitor voltage and inductor current for DET, SSA, GAM and SGAM model in dc-dc converters are calculated in interval from 0.09956 to 0.1 (buck) and from 0.39965 to 0.4(boost) as shown in Table 4.2 and 4.6.

4.1.1 Boost Converter Simulation Results

The simple boost converter as shown Fig.2.1 is used to describe the SGAM method. The parameters that have been used are listed in Table 4.1. The load resistance undergoes a step from 21Ω to 42Ω at $t = 0.2$ sec. The step load resistance changes impact on the capacitor voltage and the inductor current in all models that have been built. The inductor current and the capacitor voltage for a SGAM model of order 0, 1c, 1s are illustrated in Fig.4.1 and 4.2 . The zeroth-order

SGAM starts to oscillate and then becomes stable. when the step load resistance is changed its value, the capacitor voltage returns oscillated and become stable after a while. The cosine- and sine-orders start to oscillate and then settle close to zero. The SGAM orders refer to the dc- fundamental and the switching harmonics to estimate the average behavior and ripple behavior for the dc-dc converters.

Table 4.1: The Parameters of Boost Converter

Input Voltage, V_{in2}	125 V Boost Con
Inductance, L	1.52 mH
Capacitor, $C2$	470 μF
Switching Frequency, f_{sw}	10 kHz
ω	62832, ($2\pi f_{sw}$)
α	628320, 10ω
Initial Load Resistance, R_{L2}	21 Ω
Final Load Resistance, R_{L2}	42 Ω
Load Step Time	0.05 s
Duty Cycle, $D2$	0.4

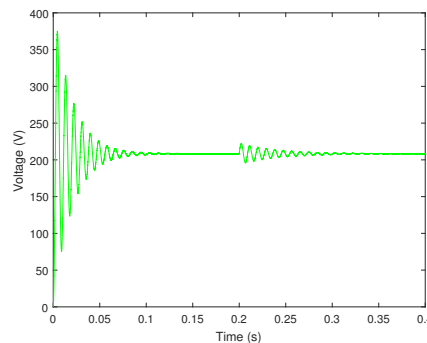


Figure 4.1: The Capacitor voltage for SGAM model in boost converter

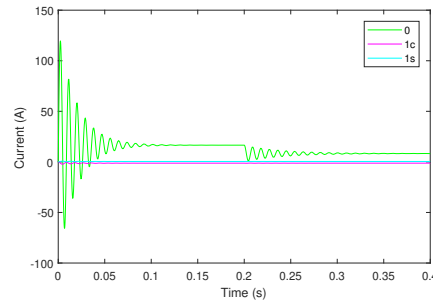


Figure 4.2: The inductance current for SGAM model in boost converter

The DET, SSA, and SGAM model are compared as shown in Fig. 4.3 and 4.4. The capacitor voltage and inductance current for SSA are approximated matched. Also, these state variables are matched when the load resistance change.

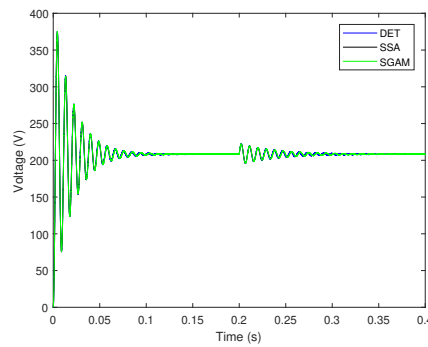


Figure 4.3: The capacitor voltage for detailed, SSA SGAM in boost converter

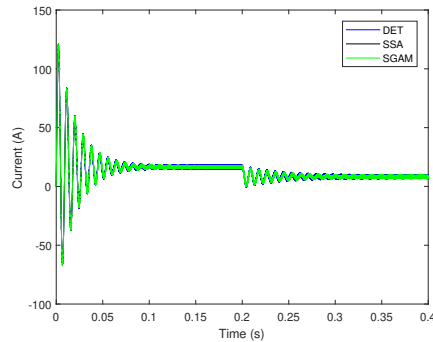


Figure 4.4: The inductance current for detailed, SSA SGAM in boost converter

However, when the capacitor voltage and inductance current for the DET, SSA, and SGAM are zoomed for the last period, these models are oscillated around the stable SSA capacitor voltage as shown in Fig. 4.5 and 4.6. the same way with inductance current for these models. The SSA method does not present the switching ripple. The SSA method shows the dc capacitor voltage and inductance current

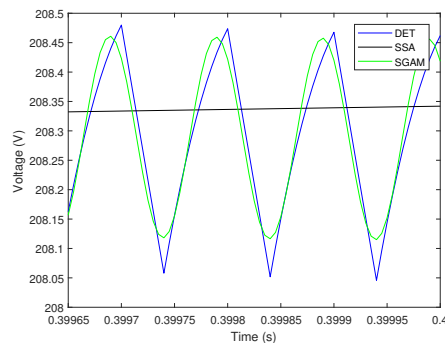


Figure 4.5: The capacitor voltage for Detailed,SSA,and SGAM models in boost converter

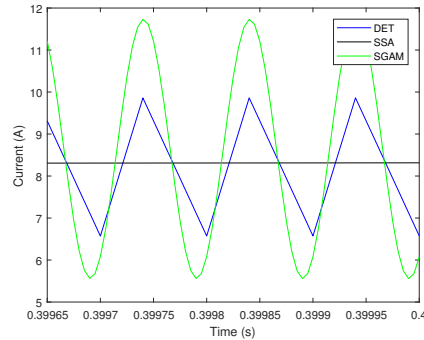


Figure 4.6: The inductor current for Detailed,SSA,and SGAM models in boost converter

In Fig. 4.7 and 4.8, the SGAM model is compared with GAM model. The capacitor voltage and inductance current of order 0, 1c, 1s for SGAM are approximately identical to the capacitor voltage of order 0, 1c, 1s for GAM, respectively. The inductance current for GAM also matches the inductance current for SGAM method. As described before, when the load resistance change occurs, the state variables return to oscillate and become stable after a while

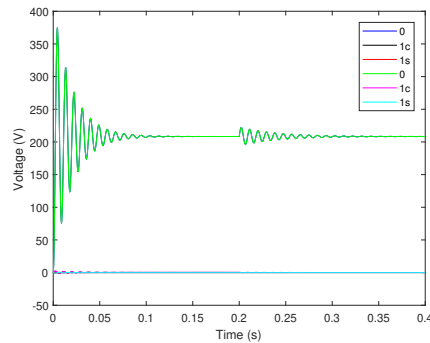


Figure 4.7: The Capacitor voltage for GAM and SGAM model in boost converter

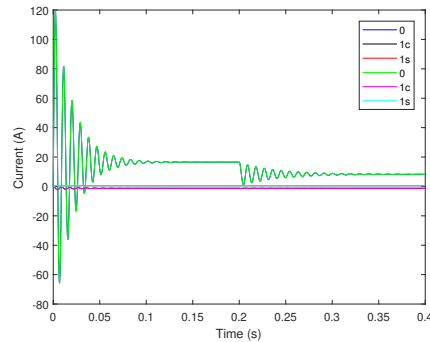


Figure 4.8: The inductance current for GAM and SGAM models in boost converter

In Fig. 4.9 and 4.10, The capacitor voltage and inductance current for the GAM are a little higher than the capacitor voltage and inductance current for SGAM while these models are zoomed in.

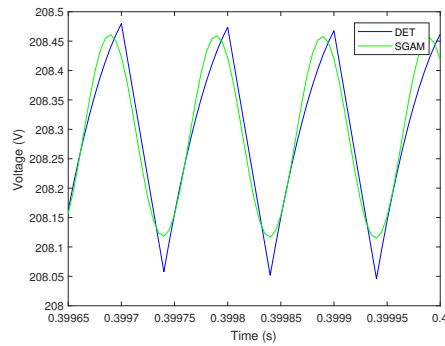


Figure 4.9: The capacitor voltage for GAM and SGAM models in boost converter

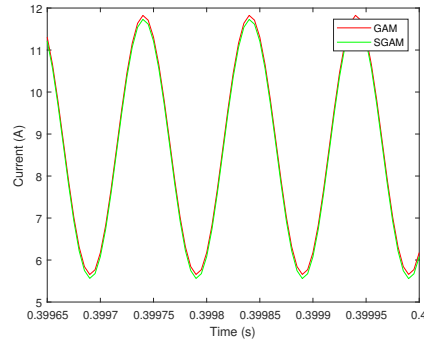


Figure 4.10: The inductor current for GAM and SGAM models in boost converter

The run time simulation of the boost converter is shown in Table 4.2. The run time simulation takes the longest time from SSA, GAM, and SGAM models. The SGAM model faster than DET run time. Table 4.3 illustrates the comparison dc values and peak to peak (P-P) of capacitor voltage and inductor current for DET, SSA, GAM, and SGAM model in boost converters in the interval from 0.09956 to 0.1 sec.

Table 4.2: Run time simulation for boost converter

Model	Run Time (s)
Detailed	2.8317
SSA	0.4045
GAM	0.7130
SGAM	0.7372

Table 4.3: Comparison of DC value and peak-peak (P-P) value of inductor current and capacitor voltage for detailed DET, SSA, GAM, and SGAM models of boost converter

Model	Inductance Current Boost Con		Capacitor Voltage Boost Con	
	DC	P-P	DC	P-P
DET	19.0339	3.9505	208.3609	0.4222
SSA	8.2414	0.0000	208.4323	0.0000
GAM	8.7418	6.1680	208.3137	0.3489
SGAM	8.6427	6.1690	208.2858	0.3411

4.1.2 Buck Converter Simulation Results

The ideal buck converter as shown Fig. 2.3 is employed to describe the SGAM method. The parameters that have been used are listed in Table 4.4.

Table 4.4: Buck Converter Simulation Parameters

	250 V Buck Con
Input Voltage, V_{in1}	250 V Buck Con
Inductance, L	1.52 mH
Capacitor, $C1$	167 μF
Switching Frequency, f_{sw}	10 kHz
ω	62832, $(2\pi f_{sw})$
α	628320, 10ω
Initial Load Resistance, R_{L1}	4 Ω
Final Load Resistance, R_{L1}	8 Ω
Load Step Time	0.05 s
Duty Cycle, $D1$	0.6

A unit step load resistance change is studied. The step load resistance change is affected on the capacitor voltage and the inductance current in all models that have been built. The capacitor voltage and

the inductor current and for a SGAM model of order 0, $1c$, $1s$ are illustrated in Fig.4.11 and 4.12. The zeroth-order SGAM starts to oscillate and then becomes stable. When the step load resistance is changed its value, the inductance current starts to oscillate and then becomes stable. The inductance current value becomes less half its value than before the resistance change. However, the capacitor voltage experiences transient and becomes stable. When the step load resistance is changed its value, the capacitor voltage returns oscillated and become stable after a while. The cosine and sine- orders start to oscillate and then settle close to zero.

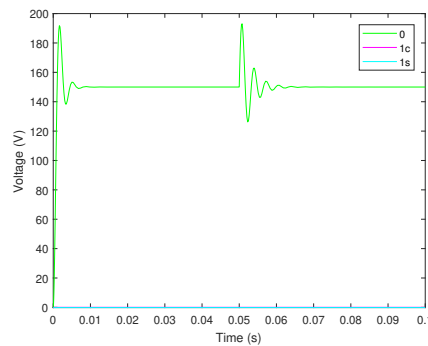


Figure 4.11: The capacitor voltage of SGAM in buck converter

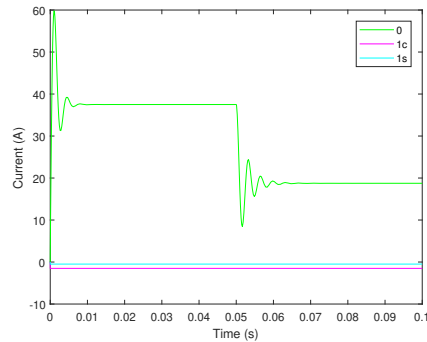


Figure 4.12: The inductance current of SGAM in buck converter

The SGAM method is compared with a detailed model as shown in Fig.4.13 and Fig.4.14. The capacitance voltage and the inductance current detailed model match the capacitance voltage and inductance current of SGAM model, respectively.

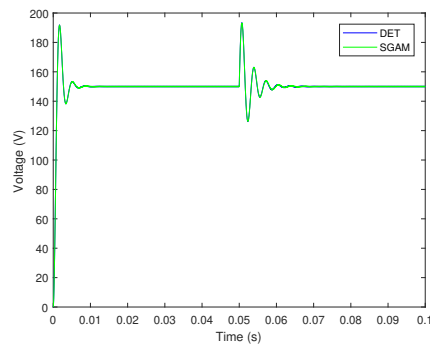


Figure 4.13: Capacitor voltage of SGAM and DET model in buck converter

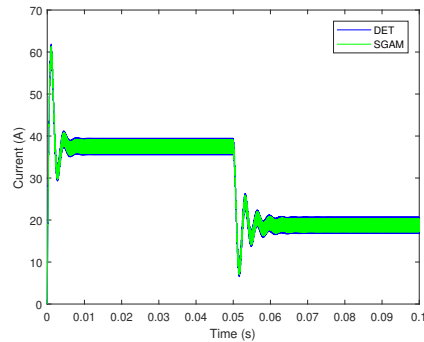


Figure 4.14: Inductor current of SGAM and DET model in buck converter

However, when these outputs are zoomed in, the capacitor voltage for DET model is a little higher than the capacitor voltage for SGAM as shown Fig. 4.15. The inductance current of DET is also higher than the inductance current of SGAM as shown in 4.16.

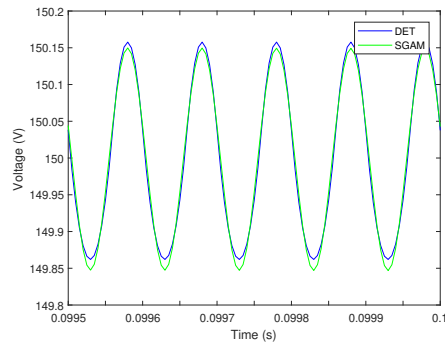


Figure 4.15: Capacitor voltage of SGAM and DET model in buck converter

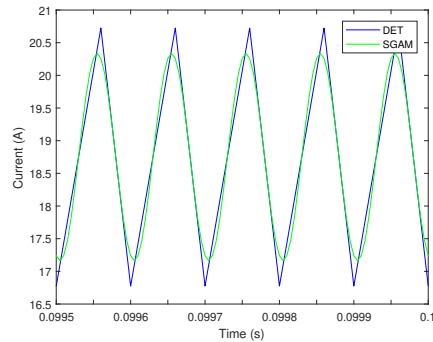


Figure 4.16: Inductance current of SGAM and DET model in buck converter

In Fig. 4.17 and Fig. 4.18, the capacitor voltage and inductance current for SSA is just dc fundamental and does not present the harmonic signals, however, the capacitor voltage and inductance current for SGAM oscillates around the capacitor voltage and inductance current of SSA.

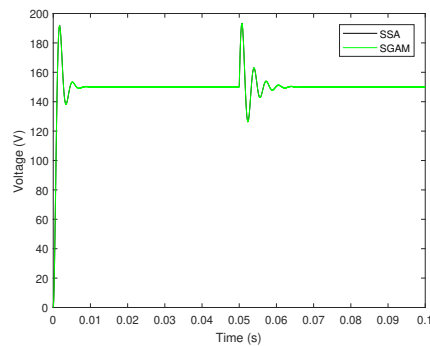


Figure 4.17: Capacitor voltage of SGAM and SSA models in buck converter

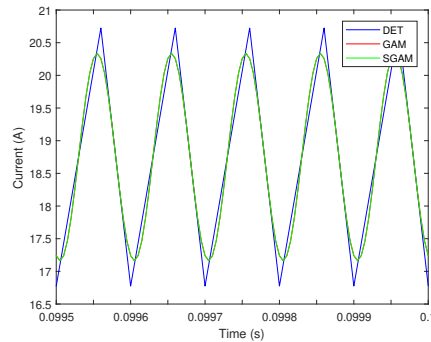


Figure 4.18: Inductance current of SGAM, DET, and GAM models in buck converter

In Fig. 4.20, the SGAM model is compared with GAM model. The capacitor voltage of order 0,1c,1s for SGAM, are identical to the capacitor voltage of order 0,1c,1s for GAM, respectively. Similarly, the inductance current for SGAM also matches identically the inductance current for GAM models as shown in Fig. 4.19.

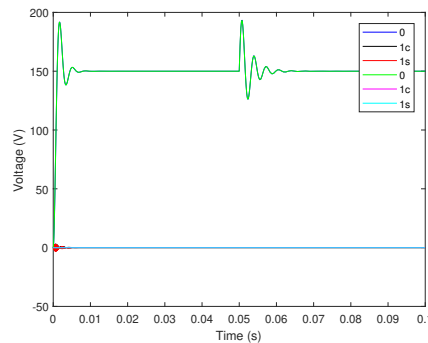


Figure 4.19: The capacitor voltage for SGAM and GAM model in buck converter

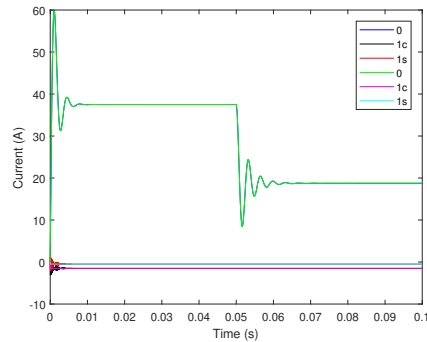


Figure 4.20: Inductance current for SGAM and GAM model in buck converter

However, when using zoom the capacitor voltage and inductance current as shown in Fig. 4.21 and 4.22, the inductance current for GAM and SGAM are identical, but the inductance current for DET oscillate a little higher than the inductance current GAM and SGAM. As described before, when the load resistance changes occur, the magnitude of inductance current and capacitance voltage decrease to the half with oscillated conditions because the load resistance value is changed and affects on state variables.

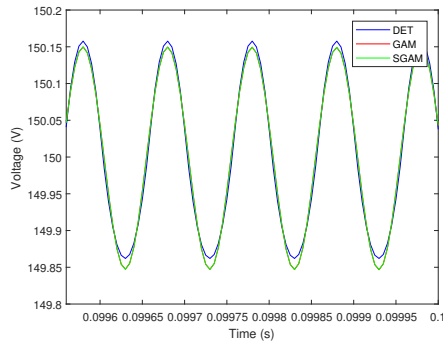


Figure 4.21: Capacitor voltage for DET,GAM and SGAM models in buck converter

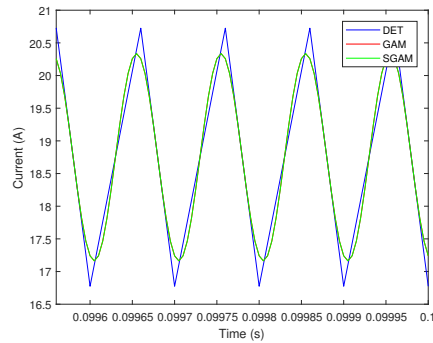


Figure 4.22: Inductance current for DET, GAM, and SGAM models in buck converter

In Fig. 4.24 and 4.23, the capacitor voltage for DET, GAM and SGAM are approximately identical. The capacitance voltage and inductance current for DET is approximated identical to the capacitance voltage and inductance current, respectively.

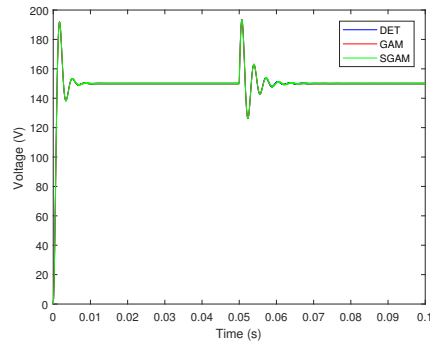


Figure 4.23: Capacitor voltage for DET, GAM, and SGAM model in buck converter

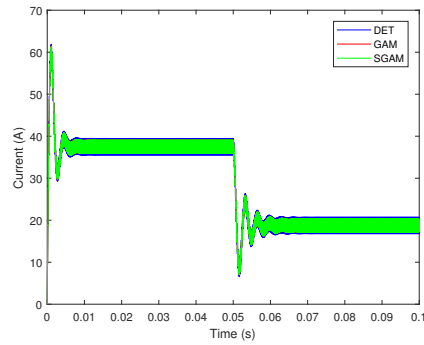


Figure 4.24: Inductance current for DET, GAM, and SGAM models in buck converter

Table 4.5: Run Time Simulation of Boost Converter

Model	Run Time buck (s)
Detailed	0.6883
SSA	0.2637
GAM	0.3001
SGAM	0.3663

Table 4.6: Comparison of dc value and peak-peak (P-P) value of inductor current and capacitor voltage for detailed, SSA, GAM, and SGAM models

Model	Inductance Current Buck Con		Capacitor Voltage Buck Con	
	DC	P-P	DC	P-P
DET	19.0339	3.9505	149.9905	0.2957
SSA	37.500	0.0000	150.0000	0.0000
GAM	18.7497	3.1730	149.9978	0.3022
SGAM	18.7503	3.1730	149.9980	0.3023

Chapter 5

Discussion and Conclusions

5.1 Discussion The Results for The Models

The SGAM model has been designed and implemented in dc-dc converters using Matlab Simulink. This model has been compared with other models such as DET, SSA, and GAM models. First, DET model, since the capacitor voltage and inductor current of SGAM is approximated identically to capacitor voltage and inductor current of DET as shown in Fig. 4.13 and 4.16, the SGAM method can illustrate the actual signal behavior in the boost and buck converters. That because the DET model is able to depict each switch behavior in the dc-dc converters[28]. Second, SSA model, according to the results of SGAM and SSA methods in Fig. 4.5 and 4.6, the capacitor voltage and inductor current for SGAM does not match the capaci-

tor voltage and inductor current for SSA in both dc-dc converters. It observes that the capacitor voltage and inductor current becomes dc and never oscillate and the capacitor voltage and inductor current for SGAM are still oscillated. These results attribute that SSA method does not present the ripple behavior, and the SGAM is more accurate and has ability to predict the average and ripple behavior[15]. Third, GAM, the capacitor voltage and inductor current for SGAM are precisely identical to capacitor voltage and inductor current for GAM as shown in Fig. 4.9 and 4.10. In addition, the SGAM is more appropriate method than GAM model because the Lyapunov function in SGAM model improved the stability of the system internally, see equations 3.42. This function utilized a positive in the SGAM integer and negative derivative. Furthermore, SGAM method also stable in the buck and boost converters due to using the S-plane method, Fig. 3.5 and Fig.3.6 , the poles and zeros of SGAM model lie in the left-hand side and the eigenvalues are less than zero [49–52] While, GAM has only one pair of eigenvalues in the right plane which makes it unstable [44]. The Kronecker product is also

used to assist the multiplying the matrices that have different sizes (dimensions)[46–48]. In terms of integrator comparison between the SGAM and GAM models, the results in fig. (integrator) utilize that the elements of dc and ripple signal of the SGAM ($0, 1c, 1s$) experience transient and became stable because of α parameter in the integrator matrix. This parameter is a flexible to be adjusted to obtain the stable system. The SGAM method takes reasonable run time simulation compared to DET model in boost and buck converters. Although the SGAM integrator is more complicated structure (more than matrix) compared to GAM, the SGAM runtime simulation is close to the run time of GAM. The SSA model takes the lower run time simulation compared to SGAM run time because the SSA integrator is simpler than the SGAM integrator. As mentioned earlier, the SGAM can estimate the average and ripple behavior and SSA method does not.

5.2 Conclusions and Future Work

SGAM has been used in dc-dc converters and compared with other models. The SGAM is more straightforward implementation

than other models. The SGAM represents a suitable alternative to DET models when high accuracy simulations are desired without long simulation run times. The SGAM does not have many restrictions and has constant equilibrium and internal stability. It is developed through MATLAB/Simulink, and Lyapunov theory has been used to prove the stability of the system. This model is capable of predicting the ripple and average behavior dc-dc converter. Future work can extend the SGAM method to other converters, including ac-dc, dc-ac converters, and different types of dc-dc converters such as buck-boost converters. Also, it can be applied SGAM in hardware in the lab. We can notice the SGAM in the practical dc-dc converter which means what the ESR impact on the output capacitor voltage and inductor current.

Appendix A

Hardware DC-DC Converter in The Lab

Figure 1 shows the hardware converter in the lab. This converter can be adjusted the dc voltage source (high or low voltage) to use it boost or buck converter.

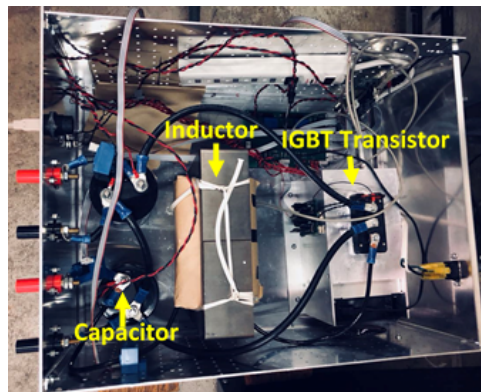


Figure 1: The converter hardware

Figure 2 illustrates the input voltage ports for the dc-dc converter.

It connects to the source voltage.

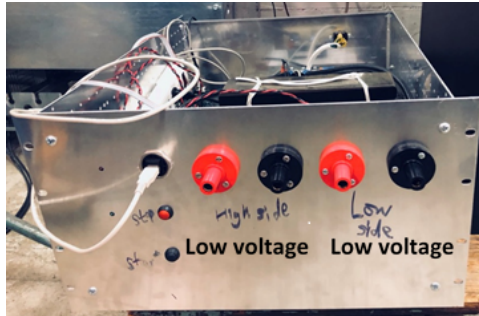


Figure 2: The input ports in converter hardware

Figure 3 shows the load resistance that have used in dc-dc converter.



Figure 3: The load resistance hardware

References

- [1] S. Chakraborty, M. G. Simoes, and W. E. Kramer, “Chapter 2 -fundamentals of power electronics,” in *Power Electronics for Renewable and Distributed Energy Systems*. London: Springer, 2013, pp. 7 – 59.
- [2] D. M. Bellur and M. K. Kazimierczuk, “DC-DC converters for electric vehicle applications,” in *IEEE Electrical Insulation Conference and Electrical Manufacturing Expo, 2007*, pp. 286–293.
- [3] Z. Yang, J. Qu, YingchuanMa, and X. Shi, “Modeling and simulation of power distribution system in more electric aircraft,” *Hindawi Publishing Corporation*, vol. 2015, pp. 1–7, November 2015. [Online]. Available: <http://dx.doi.org/10.1155/2015/847624>
- [4] S. Masri and P. W. Chan, “Design and development of a DC-DC boost converter with constant output voltage,” in *2010 International Conference on Intelligent and Advanced Systems*. IEEE, September 2011, pp. 234–245.

- [5] S. Koziel, L. Leifsson, I. Couckuyt, and T. Dhaene, “Reliable reduced cost modeling and design optimization of microwave filters using cokriging,” *International Journal of Numerical Modelling: Electronic Networks, Devices and Fields*, pp. 493–505, September 2013.
- [6] A. Ghosh and M. Kandpal, “State-space average modeling of dc-dc converters with parasitic in discontinuous conduction mode (dcm),” *Rourkela*, 2010.
- [7] S. Sanders, J. Noworolski, X. Liu, and G. Verghese, “Generalized averaging method for power conversion circuits,” in *IEEE Power Electronics Specialists Conference*, vol. 6, April 1991, pp. 251 – 259.
- [8] A. Alvarez, J. R. Melgoza, J. Juan, and R. Pasaye, “Exact steady state analysis in power converters using floquet decomposition,” *North American Power Symposium (NAPS)*, pp. 1–7, 2011.
- [9] D. Aeyels, “Asymptotic stability of nonautonomous systems by liapunov’s direct method,” vol. 25, no. 4, September 1994.
- [10] C. S. Sachin and S. G. Nayak, “Design and simulation for sliding mode control in DC-DC boost converter,” in *2017 2nd International Conference on Communication and Electronics Systems (ICCES)*. IEEE, 2018.

- [11] D. Maksimovic, A. Stankovic, V. Thottuvelil, and G. Verghese, "Modeling and simulation of power electronic converters," in *Proceedings of the IEEE*, vol. 89, no. 6. IEEE, June 2001, pp. 898–912.
- [12] H. Mahmood and K. Natarajan, "Parasitics and voltage collapse of the dc-dc boost converter," in *2008 Canadian Conference on Electrical and Computer Engineering*. IEEE, May 2008, pp. 273–278.
- [13] D. A. Torrey and U. S. Selamogullari, "A behavioral model for DC-DC converters using modelica," in *International Modelica Conference*, March 2002, pp. 167–172.
- [14] V. Caliskan, G. Verghese, and A. Stankovic, "Multi-frequency averaging of DC/DC converters," in *5th IEEE Workshop on Computers in Power Electronics*. IEEE, August 2002, pp. 124–133.
- [15] R. H. Tan and L. Y. H. Hoo, "DC-DC converter modeling and simulation using state space approach," in *2015 IEEE Conference on Energy Conversion (CENCON)*. IEEE, February 2016, pp. 42–47.
- [16] D. Maksimovic, A. Stankovic, V. Thottuvelil, and G. Verghese, "Modeling and simulation of power electronic converters," in *Proceedings of the IEEE*, vol. 89, no. 6. IEEE, January 2001.

- [17] G. V. Silva, R. F. Coelho, and T. B. Lazzarin, "State space modeling of a hybrid switched-capacitor boost converter," in *2015 IEEE 13th Brazilian Power Electronics Conference and 1st Southern Power Electronics Conference (COBEP/SPEC)*. IEEE, February 2016.
- [18] A. Davoudi, J. Jatskevich, and T. D. Rybel, "Numerical state-space average-value modeling of PWM DC-DC converters operating in DCM and CCM," *IEEE Transactions on Power Electronics*, vol. 21, no. 4, July 2006.
- [19] M. R. Modabbernia, A. R. Sahab, M. Taghy, Mirzaee, and K. Ghorbany, "The state space average model of boost switching regulator including all of the system uncertainties," *IEEE Transactions on Power Electronics*, pp. 3476–3483, July 2012.
- [20] J. Mahdavi, A. Emadi, and H. Toliyat, "Application of state space averaging method to sliding mode control of pwm dc/dc converters," *IEEE Industry Applications Society*, pp. 820–827, October 1997.
- [21] Y. Qiu, M. Xu, K. Yao, J. Sun, and F. Lee, "The multi-frequency small-signal model for buck and multiphase interleaving buck converters," in *Twentieth Annual IEEE Applied Power Electronics Conference and Exposition*. IEEE, June 2005, pp. 392–398.
- [22] S. R. Sanders, J. M. Noworolski, X. Z. Liu, , and G. C. Vergh-

- ese, “Generalized averaging method for power conversion circuits,” in *Twentieth Annual IEEE Applied Power Electronics Conference and Exposition*. IEEE, June 2005.
- [23] X. Yang, V. Smaluk, L. Yu, and K. H. Y. Tian, “Multi-frequency AC loco: A fast and precise technique for lattice correction,” pp. 831–834, June 2005.
- [24] H. Behjati, L. Niu, A. Davoudi, and P. L. Chapman, “Alternative time-invariant multi-frequency modeling of PWM DC-DC converters,” *IEEE Transactions on Circuits and Systems*, vol. 60, no. 11, pp. 3069 – 3079, July 2013.
- [25] F. Pan and A. M. Cramer, “Reduced-order multifrequency averaging in naturally sampled PWM converters,” in *Energy Conversion Congress and Exposition (ECCE), 2014 IEEE*, no. 8. IEEE, February 2014, pp. 3010–3015.
- [26] Y. Chen, A. Davoudi, and P. L. Chapman, “Multifrequency modeling of a multiple-input DC-DC converter,” in *IEEE Power Electronics Specialists Conference*, August 2008.
- [27] J. A. Peacock, *Fourier Analysis*, 2013.
- [28] X. Liu, A. M. Cramer, and F. Pan, “Generalized average method for time-invariant modeling of inverters,” *IEEE Transactions on Circuits and Systems*, vol. 64, no. 3, pp. 740–751, 2017.

- [29] P. L. C. Yongxiang Chen, Ali Davoudi, “Multifrequency modeling of a multiple-input dc- dc.”
- [30] R. Allan, A. L. da Silva, A. Abu-Nasser, and R. Burchett, “Discrete convolution in power system reliability,” *IEEE Transactions on Reliability*, vol. 30, no. 5, pp. 452–456.
- [31] S. D. Favero, “Linear time periodic analysis of dc-dc converter,” *IEEE Transactions on Reliability*, no. 5, June 2006.
- [32] A. Yazdani and R. Iravani, “A generalized state-space averaged model of the three-level npc converter for systematic DC-voltage-balancer and current-controller design,” *IEEE Transactions on Power Delivery*, vol. 20, pp. 1105 – 1114, April 2005.
- [33] B. Lehman and R. Bass, “Switching frequency dependent averaged models for PWM DC-DC converters,” *IEEE Transactions on Power Electronics*, vol. 11, no. 1, pp. 89–98, January 1996.
- [34] A. Emadi, “Modelling and analysis of multi-converter DC power electronic systems using the generalized state space averaging method,” in *IECON’01. 27th Annual Conference of the IEEE Industrial Electronics Society*, August 2002.
- [35] P. N. Enjeti, P. D. Ziogas, and J. F. Lindsay, “Programmed PWM techniques to eliminate harmonics: A critical evaluation,” *IEEE Transactions on Industry Applications*, vol. 26, no. 2, pp. 302–316, April 1990.

- [36] A. Prasad, P. Ziogas, and S. Manias, “A three-phase resonant PWM DC-DC converter,” pp. 463–473, 1991.
- [37] Y. Fuad, W. L. de Koning, and J. W. van der Woude, “Pulse-width modulated DC-DC converters,” *International Journal of Electrical Engineering Education*, vol. 38, no. 1, pp. 54–79, 2001.
- [38] E. van Dijk, H. J. N. Spruijt, D. M. O’Sullivan, , and J. B. Klaassens, “PWM-switch modeling of DC-DC converters,” *IEEE Transactions on Industry Applications*, vol. 10, no. 6, pp. 659–665, November 1995.
- [39] V. Raviand, K. Kanamarlapudi, S. Ping, and S. Lam, “Analysis and implementation of pulse-width modulated DC-DC converter for electric vehicles with improved efficiency,” in *2016 IEEE International Conference on Power Electronics, Drives and Energy Systems (PEDES)*. IEEE, December 2016.
- [40] G. S. Deaecto and J. C. Geromel, “Stability analysis and control design of discrete-time switched affine systems,” *IEEE Transactions on Automatic Control*, vol. 62, no. 8, pp. 4058 – 4065, AUGUST 2017.
- [41] A. Emadi, A. Khaligh, C. Rivetta, and G. Williamson, “Constant power loads and negative impedance instability in automotive systems: definition, modeling, stability, and control of power electronic converters and motor drives,” *IEEE Transac-*

tions on Vehicular Technology, vol. 55, no. 4, pp. 1112–1125, July 2006.

- [42] B. P. Loop, S. D. Sudhoff, S. H. Zak, and E. L. Zivi, “Estimating regions of asymptotic stability of power electronics systems using genetic algorithms,” *IEEE Transactions on Control Systems Technology*, vol. 18, no. 5, pp. 1011–1022, September 2010.
- [43] J. Daafouz, P. Riedinger, and C. Iung, “Stability analysis and control synthesis for switched systems: a switched lyapunov function approach,” *IEEE Transactions on Control Systems Technology*, vol. 47, no. 11, pp. 1883 – 1887, November 2002.
- [44] F. Pan, “Multifrequency averaging in power electronic systems,” PhD dissertation, University of Kentucky, 2014.
- [45] F. Misoc, M. M. Morcos, and J. Lookadoo, “Fourier-series models of DC-DC converters,” in *2006 38th North American Power Symposium*, May 2007.
- [46] A. Laub, “Chapter 3 -kronecker products,” in *Matrix Analysis for Scientists and Engineers*. The Society for Industrial and Applied Mathematics, 2005, pp. 150 – 158.
- [47] J. Brewer, “Kronecker products and matrix calculus in system theory,” *IEEE Transactions on Circuits and Systems*, vol. 25, no. 9, pp. 772–781, September 1978.

- [48] C. Loan, “The ubiquitous kronecker product,” *Journal of Computational and Applied Mathematics*, pp. 85–100, October 2000.
- [49] T. K. . M. Nagurka, “Understanding the root locus using gain plots,” *IEEE Control Systems*, vol. 11, no. 5, pp. 37–40, August 1991.
- [50] J. Aseltine, “On the synthesis of feedback systems with open-loop constraints,” *IRE Transactions on Automatic Control*, vol. 4, no. 1, pp. 31–37, May 1959.
- [51] T. Cavicehi, “Phase-root locus and relative stability,” *IEEE Control Systems*, vol. 16, no. 4, pp. 69–77, August 1996.
- [52] J. Zaborszky, “Integrated s-plane synthesis using 2-way root locus,” *Transactions of the American Institute of Electrical Engineers, Part I: Communication and Electronics*, vol. 75, pp. 797 – 801, January 1957.

VITA

Mahsen S. Al-Ani

EDUCATION

University of Kentucky

2018, Master of Science- Electrical and Computer Engineering

2016, Student in English as Second Language (ESL) institute

University of Technology, Iraq

2006, Bachelor of Science in Electrical and Computer Engineering

EXPERIENCE

University of Kentucky

2018, Teaching Assistant, College of Engineering

2017, UK Solar Car Team, University of Kentucky

University of Technology, Iraq (2008-2013)

Engineer in Analog Electronics lab

Engineer in Microprocessor 8085 lab

Engineer in Control lab

Engineer in MATLAB lab

INTERNATIONAL PROFESSIONAL MEMBERSHIPS

Institute of Electrical and Electronics Engineers (IEEE)

Society of Women Engineers (SWE)

SERVICE/AWARDS

Service

2014, Academic Team in Glendover Elementary School

2017, ESL Students in Glendover Elementary School

2017, Career Fair 2017 in University of Kentucky

Awards/Certificates

2018, Best Presentation in Feeder Summer Institute "Transactive Power Flow"

2017, Power and energy Institute of Kentucky

2017, Lean System Program, Institute of Research for Technology Development, University of Kentucky

2018, Feeder Summer Institute on Transactive Power Flow, University of South Carolina, Columbia, SC

Travelling Awards

2017, Student travel award to SWE conference, Pittsburgh, PA

2018, Student travel award to SWE conference, Cliffview, KY

Out of the University of Kentucky

2011, Recognition Thanks, University of Technology

ABSTRACT/PRESENTATION

University of Kentucky

M. Al-Ani, A. Cramer "Stability Improvements for Generalized Average-Value Model of DC-DC Converter", 1st Annual ECE Student Research Symposium, University of Kentucky, Lexington, KY, 2018.

M. Al-Ani, M. Biswas, O. Akeyo, S. Reese, S. Witsell "Hot House Team in Transactive Power Flow Institute", University of South Carolina.

Publication Out of the University of Kentucky

Assisted in publishing the quire of C++ programming guide, University of Technology.

Assisted in publishing the quire electronic circuits, university of Technology.